

1 Late Holocene palaeoenvironmental records from the
2 Anzali and Amirkola Lagoons (south Caspian Sea):
3 vegetation and sea level changes
4

5 Leroy S.A.G.^{a*}, Lahijani H.A.K.^b, Djamali M.^c, Naqinezhad A.^d, Moghadam
6 M.V.^e, Arpe K.^{fa}, Shah-Hosseini M.^b, Hosseindoust M.^b, Miller Ch.S.^{a1},
7 Tavakoli V.^{bg}, Habibi P.^b and Naderi M.^b

8
9 a Institute for the Environment, Brunel University, Kingston Lane, Uxbridge UB8 3PH, West
10 London, UK, suzanne.leroy@brunel.ac.uk, tel +44-1895-266 087, fax: +44-1895-269 761.

11 b Iranian National Institute for Oceanography (INIO), No. 3, Etemadzadeh St., Fatemi Ave.,
12 Tehran 1411813389, Iran, lahijani@inco.ac.ir, hamidaki@yahoo.com, shmajid@gmail.com,
13 hdsal_1980@yahoo.com, phabibi@inco.ac.ir and majid.naderi@gmail.com

14 c Institut Méditerranéen d'Ecologie et de Paléocécologie (IMEP UMR CNRS 6116, Europôle
15 Méditerranéen de l'Arbois, Bâtiment Villemin BP 80, 13545 Aix-en-Provence CEDEX 04,
16 France, morteza_djamali@yahoo.com

17 d Department of Biology, Faculty of Basic Sciences, University of Mazandaran, P. O. Box:
18 47416-95447, Babolsar, Mazandaran, Iran, a.naqinezhad@umz.ac.ir and
19 anaqinezhad@gmail.com.

20 e Department of Physics, Faculty of Sciences, University of Guilan, P.O. Box 3489, Rasht,
21 Iran, mvmoghaddam@gmail.com

22 f Max Plank Institute for Meteorology, Hamburg, Germany, klaus.arpe@zmaw.de

23 g Department of Geology, College of Science, University of Tehran, Iran.
24 vahid6105@yahoo.com

25

26 * corresponding author

27 **Abstract**

28 Two internationally important Ramsar lagoons on the south coast of the
29 Caspian Sea (CS) have been studied by palynology on short sediment cores
30 for palaeoenvironmental and palaeoclimatic investigations. The sites lie within
31 a small area of very high precipitation in a region that is otherwise dry.
32 Vegetation surveys and geomorphological investigations have been used to
33 provide a background to multidisciplinary interpretation of the two sequences
34 covering the last four centuries. In the small lagoon of Amirkola, the dense
35 alder forested wetland has been briefly disturbed by fire, followed by the
36 expansion of rice paddies from AD1720 to 1800. On the contrary, the
37 terrestrial vegetation reflecting the diversity of the Hyrcanian vegetation
38 around the lagoon of Anzali remained fairly complacent over time. The
39 dinocyst and non-pollen palynomorph assemblages, revealing changes that
40 have occurred in water salinity and water levels, indicate a high stand during
41 the late Little Ice Age (LIA), from AD <1620 to 1800-1830. In Amirkola, the
42 lagoon spit remained intact over time, whereas in Anzali it broke into barrier
43 islands during the late LIA, which merged into a spit during the subsequent
44 sea level drop. A high population density and infrastructure prevented
45 renewed breaking up of the spit when sea level reached its maximum (AD
46 1995). Similar to other sites in the region around the southern CS, these two
47 lagoonal investigations indicate that the LIA had a higher sea level as a result
48 of more rainfall in the drainage basin of the CS.
49

50 **Key words (max 6 key words)**

51 Little Ice Age; pollen; dinocysts; sea level; vegetation; Caspian Sea

52

53 1 present address: Department of Earth and Environmental Sciences, CEPSAR, The Open
54 University, Walton Hall, Milton Keynes, MK7 6AA, UK, c.s.miller@open.ac.uk

55

56 1. Introduction

57 Over the period of instrumental measurements, the Caspian Sea has
58 experienced a full sea-level cycle, i. e. a rise and a fall, of around 3 m
59 (Rodionov, 1994; Kroonenberg et al., 2000), whilst global sea level rose by
60 approximately 2 mm per year (Warrick, 1993). Rapid changes in the Caspian
61 Sea (CS) level offer a unique opportunity to study global environmental
62 changes, considering the CS as a small-scale model of the world ocean
63 (Kroonenberg et al., 2000). The increasing demands for development of
64 human activities in the coastal areas reinforce the necessity for unravelling
65 the history of sea-level fluctuations (Leroy et al., 2010). Records of the CS-
66 level changes have been discovered both offshore and in coastal sediments
67 (Rychagov, 1997; Leroy et al., 2007). On the basis of these studies, some
68 CS-level curves have been reconstructed. These proposed curves are very
69 different and, to some extent, contradictory, even for a period as recent as the
70 Little Ice Age (Kroonenberg et al., 2007; Lahijani et al., 2009).

71 The Iranian coast of the CS is located on the southern part of the South
72 Caspian sub-basin (Fig. 1). Due to sea level rise, strong littoral drifts and a
73 large influx of sediment transported by rivers, coastal lagoons have developed
74 in the Central Guilan (Gilan) and East Mazandaran (Mazandaran) provinces
75 (Lahijani et al., 2009). These accumulative coastal regions were selected on
76 the basis of previous investigations indicating the need to obtain reliable sea-
77 level signatures (Zenkovich, 1957; Lahijani, 1997). In general, coastal lagoons
78 are infilled with sediment during sea level fall and submerged when sea level
79 rises (Lahijani et al., 2009). The present investigation focuses on two lagoons
80 in the province of Guilan: Amirkola and Anzali. These two lagoons are
81 enclosed by split enlargements. As they are transitional environments, these
82 coastal lagoons currently receive inflow from small rivers and irrigation water
83 prior to entering the sea. Previous work has highlighted some aspects of the
84 development of these two lagoons (Kazanci et al., 2004; Lahijani et al., 2009).
85 Palynological analyses, pollen, spores, non-pollen palynomorphs (NPPs) and
86 dinocysts, are provided here for the first time.

87 The main objective of the present study is to determine the local and
88 regional vegetation history, climatic and sea-level fluctuations, while taking
89 local coastal geomorphology into consideration.

90 2. Settings

91 2.1 Geographical setting

92 2.1.1 The Iranian coast of the Caspian Sea

93 Instrumental measurements of sea level, available since 1830, show
94 fluctuations up to 3 m resulting from a seawater imbalance, mainly the
95 difference between river influx and evaporation (Terziev, 1992). In this regard,
96 instrumental measurements (Malinin, 1994; Rodionov, 1994) and late
97 Holocene hydrological data (Varushenko et al., 1987) indicate that the Volga
98 River, in the NW of the CS, is the main contributor to sea-level fluctuations
99 (Arpe et al., 2000; Arpe and Leroy, 2007). During the past half century,
100 several studies attempted to predict sea-level fluctuations in the Caspian

101 basin. However, these studies failed to predict the sea-level rise of AD 1979
102 and the fall in AD 1995, demonstrating that the controlling factors governing
103 the water balance are not yet fully understood. [Arpe et al. \(2000\)](#) found that
104 one factor controlling the water balance in the CS is the precipitation over the
105 Volga River of which the variability is forced by ENSO. During periods of El-
106 Niño events, more precipitation occurs leading to an increase of the CS level.

107 Although it is the Volga River that provides most freshwater to the CS
108 and sediment input for the northern part of the CS, the sediment influx for the
109 southern basin is clearly mainly from Sefidrud and Kura Rivers ([Klige and
110 Selivanov, 1995](#); [Mikhailov, 1997](#); [Lahijani et al., 2008](#)). The southern Caspian
111 coast in the north of Iran is indeed characterized by high terrigenous sediment
112 flux. About 61 rivers from the Iranian Caspian coast flow to the CS along the
113 820 km of Iranian coast ([Afshin, 1994](#)). Most originate in the northern flank of
114 the Alborz, the Sefidrud (i.e. the Sefid River) having the largest catchment
115 area. At present, under intense human activities, the rivers annually supply
116 about 33 million tons of sediments and 11 km³ of water (i. e. one volume of
117 sediment in 300 volumes of water) to the shoreline in total, of which the
118 Sefidrud accounts for 80% of the sediment and 40% of the water ([Krasnozhan
119 et al., 1999](#)). Great rivers with significant sediment loads (Sefidrud in central
120 Guilan and Gorganrud in Golestan) have developed large deltas into the CS.
121 Their old deltas, along with fluviodeltaic deposits of medium-size rivers, have
122 developed a wide coastal area in the central Guilan, east Mazandaran and
123 Golestan regions ([Kousari, 1986](#); [Lahijani, 1997](#)). In particular, the coastal
124 plain of the Sefidrud is characterized by abundant distributary channels and
125 extensive flood plains, on which local swamps are common ([Kousari, 1986](#)).
126 Here, sediments with some marine characteristics are locally observed on the
127 coastal plain, which reflect temporal sea-level influence. The main channel of
128 the river flows into the CS near Kiashahr city, forming the Sefidrud delta and
129 shows high sinuosity within its alluvial valley, resulting in many abandoned
130 channels (Fig. 1). During its development history, the Sefidrud repeatedly
131 changed its course from west (Anzali) to the east (Lahijan), the last change
132 occurred around 400 yr BP ([Lahijani et al., 2009](#)), from Amirkola to Kiashahr
133 (Fig. 1). The old Sefidrud (30 km east of Kiashahr, named 'Kohneh Sefidrud'
134 in Persian) was the main channel in historic times. Seemingly, it was
135 responsible for the development of the ancient delta northeast of Lahijan
136 ([Kousari, 1986](#)).

137 Generally, longshore currents have a great effect on coastal
138 morphology ([Lahijani et al., 2009](#)). In the study area, lagoons and bays are
139 formed behind the barrier beaches, which developed in central Guilan, east
140 Mazandaran and Golestan coasts. From west to the east, Anzali, Zibakenar,
141 Kiashahr, Amirkola, Miankaleh and Gomishan are the major lagoons that are
142 separated from the CS by spits and bars ([Kousari, 1986, 1988](#); [Lahijani,
143 1997](#)). Coastal forces, mainly sea level change, wave and wave-induced
144 currents, combined with catchments' geological setting, and climate have
145 determined the sediment distribution pattern along the southern Caspian
146 coast. The modern shoreline in central Guilan is covered by sediments with a
147 sand fraction of > 95 %.

148 In brief, the Amirkola and Anzali Lagoons were probably formed during
149 the Holocene. While the Anzali Lagoon formed by littoral drift, the role of the
150 Sefidrud delta plain was to provide an eastern limit to this lagoon. The

151 Amirkola Lagoon formed by littoral drift of sediments supplied by the old
 152 Sefidrud, around AD 1600. Then, the course of Sefidrud changed, passed
 153 through a wide shallow lagoon and incised the shoreline near Kiashahr (30
 154 km west of the old mouth).
 155

156 **2.1.2 The lagoons of Amirkola and Anzali**

157 Amirkola Lagoon (also known as Amirkelayeh, Shal-e Kool and Sheikh
 158 Ali Kool) is a shallow coastal lagoon (maximum water depth of 3 m and with
 159 an average depth of 1.85 m), north of Lahijan, separated to the north by the
 160 Amirkola sandy spit from the CS (Fig. 1 and 2). It is situated at 37° 19' - 37°
 161 22' N and 50° 10' - 50° 12' E. The average altitude of this wetland is 23 m bsl
 162 relative to global sea level. The lagoon covers an area of 12.3 km². Since
 163 1970, it has been protected as a "Wildlife Refuge" by the Iranian Department
 164 of the Environment. It was also registered in the Ramsar List of Wetlands of
 165 International Importance in June 1975. A small outlet (3 m wide) permits
 166 partial unidirectional flow of the lagoonal waters to the CS. The lagoon has no
 167 river inflow and receives its freshwater by surface water passing through rice
 168 fields that surround the lagoon. The barrier is about 8 km long with an
 169 average width of 1 km. Satellite images show different steps of the prograding
 170 Amirkola beach into the CS (Lahijani et al., 2009).

171 The Amirkola Lagoon was once a part of the CS, but due to an
 172 enlargement of the Amirkola spit it has been isolated from the sea. The old
 173 Sefidrud barrier-lagoon in the Amirkola area was developed under high
 174 sediment supply of the Sefidrud and longshore currents with east-south
 175 eastward directions. Owing to a south-eastward growth of the Amirkola spit,
 176 its lagoon became entirely separated from the CS. Nevertheless, sea-level fall
 177 of the late 16th century has accelerated Amirkola Lagoon closure (Terziev,
 178 1992; Lahijani et al., 2009).

179 Since the sea-level rise in 1979, the same processes have been active
 180 in the Sefidrud delta and have formed two lagoons, i.e. Zibakenar and
 181 Kiashahr, in the west and the east of the Sefidrud, respectively (Lahijani et al.,
 182 2009).

183 The Anzali (Bandar-e Anzali, Bandar Pahlevi, Enseli and Enzelli)
 184 Lagoon, also called, Anzali Mordab and Anzali Talab (37° 26' - 37° 35' N and
 185 49° 15' - 49° 27' E) in the Guilan province (Fig. 1 and 3) is not only the largest
 186 freshwater reservoir of the southern Caspian depression, but also a famous
 187 wetland as it is one of the first certificated Ramsar sites in the world (June
 188 1975). The lagoon's maximum water depth is 5.5 m. The surface of the Anzali
 189 Lagoon and its outlet are at around 24 m bsl. It has a surface area of
 190 approximately 160 km², which fluctuates widely with sea level change. The
 191 Anzali wetland consists of three main parts: the central part near Bandar-e
 192 Anzali town, the western part and the southern part. The latter part, called
 193 Siah-Keshim, is preserved by the Department of Environment as a "protected
 194 area" and thus possesses well-protected vegetation and biodiversity. Fifteen
 195 small rivers with a catchment of 3700 km² discharge freshwater into the
 196 lagoon. The outlet is 300 m wide and allows bilateral exchange of brackish
 197 sea water and fresh lagoon water. Moreover, during storms, CS water affects
 198 the water in the outlet by mixing or causing a gradient of salinity. Moreover,
 199 when the salinity of the CS of 12.5–13.5 is taken into consideration, the water
 200 of Anzali Lagoon, excluding its central sub-basin and outlet, is typically

201 limnetic or fresh (< 0.5). More details are available in [Kazancı et al. \(2004\)](#).
 202 The phytoplankton of the Anzali Lagoon was studied in 1992, a time close to
 203 the maximal levels of 1995, alongside measurements of salinity and sulphates
 204 ([Ramezanpoor, 2004](#)). The highest salinities (10) were found in the bottom
 205 waters close to the harbour in the navigation channel, and in the east the
 206 waters were fresh but eutrophic. The influence of the CS is felt everywhere,
 207 with the harbour showing both freshwater and marine species.

208 [Kazancı et al. \(2004\)](#) have suggested that the lagoon should actually
 209 be called a lake. The lake has an evolutionary development based on coastal
 210 dynamics. The water level of the CS and coastal sands are clearly the primary
 211 factors for its development. The sands transported from the Sefidrud delta by
 212 a local westward drift probably accelerated the formation of the coastal sand
 213 ridges. The progradation of the coastal zone by the development of beach
 214 ridges was sufficiently rapid (because of sediment availability from the
 215 Sefidrud delta) that the coastal sands formed a dammed lake in a limited time.
 216 However, this mechanism is questioned by the present authors. Indeed the
 217 dominant littoral drift is from west to east and the old morphological features
 218 show the same direction. Therefore the Sefidrud simply closed the eastern
 219 part of the lagoon by fluvial and deltaic deposits and cannot have affected the
 220 beach ridges on the Anzali spit.

221 The general shape and orientation of the central Guilan coast (Anzali to
 222 Amirkola area) depend on the geographical setting. Fluvial supply from
 223 Sefidrud and other rivers in this area have been redistributed by wave and
 224 wave-induced currents. Prevailing eastward longshore currents caused the
 225 enlargement of the Anzali and Amirkola spits, which have separated these
 226 water bodies from the CS. They differ in origin from shore-parallel small
 227 lagoons that have formed due to rapid sea – level rise since 1979 ([Lahijani et
 228 al., 2009](#)).

229 **2.2 Climate**

230 Both Amirkola and Anzali Lagoons are located in an area with a warm
 231 temperate climate displaying a sub-Mediterranean character but still with
 232 some precipitation in summer. The southern Azerbaijan and the north-western
 233 Iran coasts along the CS benefit from an exceptionally wet and mild climate.
 234 Because of the general westerly flow in the middle troposphere, one might
 235 assume that the major sources of the humidity for the area are the North
 236 Atlantic, the Mediterranean and the Black Sea. However, it will be shown
 237 below that this general view must be revised. In autumn, the Siberian High
 238 becomes stronger and intensifies the north-easterly winds which sweep the
 239 surface of CS bringing considerable moisture to the southwest Caspian area.
 240 This humid air comes into contact with warm dry air masses descending from
 241 the Iranian plateau through Sefidrud gorge and a front is created at the
 242 contact zone causing an exceptionally high rainfall ([Khalili, 1973](#)). This author
 243 also found that, on the northern slopes of the Alborz, the annual precipitation
 244 decreases with altitude, and maximum rainfall occurs in the coastal plain.
 245 However the gradient of the decreasing rainfall varies between 22 and 68 mm
 246 of rain per 100 meters, which is contrary to most other places in the world.
 247 This suggests the existence of two air masses, a dry one from the Iranian
 248 plateau and a humid one from the CS, which come into contact between the
 249 mountains and the CS.

250 The results by [Khalili \(1973\)](#), which covered the period 1960 to 1969,
251 can now be extended due to the availability of more complete data sets
252 (www.irimo.ir/english). The climate of the southwest corner of the CS stands
253 out in a generally dry area with contrasting seasons (Fig. 4a). The Iranian
254 coast shows a strong gradient of annual precipitation from west to east, 2106
255 mm in Pilimbra-Nehalestan, 1860 mm in Anzali, 1379 mm in Astara and 472
256 mm in Torkaman on the SE coast; while a little further inland to the east, on
257 the slopes of the mountains, it is 620 mm in Gorgan. A very strong gradient
258 also occurs from the coast to the south, 1860 mm in Anzali, 1354 mm in
259 Rasht, 203 mm in Manjil, only 170 km south of Rasht in the valley of the
260 Sefidrud at a level of 330 m, and 313 mm in Zanjan, at a level of 1663 m asl
261 which is on the plateau of the Iranian highland. Anzali and Pilimbra-
262 Nehalestan have the highest amounts of precipitation in the region. The
263 temperatures there are mild with a coldest monthly mean temperature of 6.8
264 °C in February which can be as low as 1.2 °C in a specific year (e.g. 1972).
265 Seven days below 0 °C occur on average per year. The maximum
266 temperature is observed in July with a mean value of 26.0 °C but which
267 reached 28.2 °C in 1975.

268 The mean wind in the region is from the west (data obtained when
269 investigating the upper air circulation), especially during seasons with higher
270 precipitation. The wind for the 700 hPa level (about 3200 m above ground),
271 averaged for the period 1979 to 1999, as obtained from the ECMWF
272 reanalysis (ERA40, [Uppala et al., 2005](#)), has been investigated. The 700 hPa
273 level has been chosen here because it is low enough to carry a substantial
274 amount of moisture and high enough to show the general circulation and lies
275 above the main mountain ranges. The air descends from the Iranian plateau
276 through the Sefidrud gorge, leading to dry conditions due to the Foehn effect,
277 with the lowest precipitation, of only 203 mm per year in the area around
278 Manjil.

279 The above description applies for a large-scale view; the north Iranian
280 coast is, however, strongly influenced by local orography; this is especially
281 obvious for surface winds. The prevailing surface winds at the station Anzali
282 are from west to north in summer and north to east in winter according to
283 www.irimo.ir. In the ERA40 data, which uses a different averaging method, i.e.
284 wind components have been averaged, the wind comes more or less from the
285 north east throughout the year. This would suggest that most of the
286 precipitation around Anzali comes from the CS. Some information about the
287 origin of precipitable water can be gained by investigating time series of the
288 Anzali precipitation and the wind components at different levels. One might
289 expect that with increased westerlies at higher levels the air would descend
290 the mountain slopes towards the CS, leading to a Foehn effect, i.e. a warming
291 of the air and less precipitation. In fact one finds a significant negative
292 correlation between westerlies at 700 hPa and the precipitation at Anzali with
293 an anomaly correlation factor of -0.34. Conversely, it is expected with
294 enhanced north easterlies at lower levels that the air would rise along the
295 slopes of the mountains or when meeting the down-slope winds from the
296 Iranian plateau leading to enhanced precipitation. The anomaly correlation
297 between the two components of the winds at the surface and the precipitation
298 at Anzali are significant: -0.46 and -0.64 for the zonal and meridional
299 component respectively; so the northerly winds have the highest impact on

300 the precipitation for Anzali, probably also because these winds stay longest
 301 over the CS and can take up more moisture from the sea. This suggests that
 302 the source of moisture for the precipitation over Anzali is the CS. Knowing that
 303 the evaporation over the CS is sufficient to compensate for the inflow into the
 304 CS by all rivers, including the Volga, makes this assumption acceptable. The
 305 assumption that the precipitation around Anzali has its source over the CS is
 306 further supported by the annual cycle of evaporation over the southern CS.
 307 Like the precipitation over Anzali and neighbouring stations, shown in Fig. 4b,
 308 the maximum evaporation occurs during autumn, extending into winter,
 309 however the evaporation is leading the precipitation by perhaps 2 months.

310 The precipitation at Anzali has been investigated in this study because
 311 of the good availability of data at this locality. No station is present at
 312 Amirkola, for which the nearest station is Lahijan (further inland and therefore
 313 probably with lower precipitation amounts than Amirkola). The wind data are
 314 on a much coarser grid and can be assumed to be identical for both sites. The
 315 importance of the low-level north-easterly winds for the precipitation explains
 316 why the maximal precipitation occurs around Anzali. To the west the wind is
 317 blocked by a mountain range that runs in a north-south direction and to the
 318 south by the Alborz Mountains with an east-west direction; where the two
 319 mountain ranges converge, the air is trapped in a corner and uplifted which is
 320 where Anzali is located. According to [Khalili \(1973\)](#) the wind is not uplifted at
 321 the mountains themselves but where the dry down-slope winds from the
 322 Iranian highland plateau meet the low-level winds from the CS. This is
 323 supported by the very low precipitation rates in Manjil, half way up the
 324 mountains. It is illustrated in Fig. 4c, where south-westerlies on the highland
 325 plateau bounce against the north-easterlies from the CS on the slope of the
 326 mountains in the area SW of Anzali.

327 **2.3 Vegetation**

328 The Hyrcanian forests occur along an altitudinal and climatic gradient
 329 ranging from below sea level (vegetation 'sensitive to cold') up to 2700 m
 330 (vegetation 'resistant to cold') ([Bobeck, 1951](#); [Frey and Probst, 1986](#); [Zohary,](#)
 331 [1973](#)). The Hyrcanian vegetation extends over an area benefiting from the wet
 332 and mild climate detailed in section 2.2 ([Zohary, 1973](#)). It is characterised by a
 333 rich biodiversity and many endemics. It contains many elements of the forest
 334 that were widespread in Europe, but have disappeared during the Quaternary
 335 glaciations ([Leroy and Roiron, 1996](#)). The most striking is *Parrotia persica*, but
 336 *Pterocarya* and *Zelkova* are also genera that have seen their distribution
 337 shrinking over time ([Bobeck, 1951](#); [Meusel et al., 1965](#)). Moreover *Gleditsia* is
 338 another survival from the Tertiary.

339 Three main forest zones occur in the Hyrcanian area: lowland,
 340 submountain and mountain forest zones. Historically, the lowland Hyrcanian
 341 forest zone was characterized by a large and relatively homogenous
 342 community of Quercus-Buxetum (with *Quercus castaneifolia* and *Buxus*
 343 *hyrcana* as dominant species) that occurred across all the Caspian lowland
 344 area. Other important plant species of this community are: *Diospyros lotus*,
 345 *Gleditsia caspica*, *Albizzia julibrissin* and *Acer velutinum*. Moreover, some
 346 azonal hygrophytic vegetations including *Alnus glutinosa* subsp. *barbata* and
 347 *Pterocarya fraxinifolia* stands are also observed in this vegetation zone
 348 ([Djazirei, 1965](#); [Tregubov and Mobayen, 1970](#)) where they represent more or

349 less distinct hygrophite communities in some remnant forests ([Hamzeh'ee et al., 2008](#); [Naqinezhad et al., 2008](#)). Additionally, anthropogenic deforestation
 350 of Quercus-Buxetum resulted in the clearing of many important trees such as
 351 *Quercus castaneifolia* and *Buxus hyrcana* due to economic uses of their
 352 woods. Many original remnants of this community were naturally invaded by
 353 *Parrotia persica*, *Gleditsia caspica* and other invasive species ([Zohary, 1973](#);
 354 [Hamzeh'ee et al., 2008](#)). Historically, the lowland zones are much affected by
 355 decline due to agricultural intensification and urban development. The
 356 introduction of rice possibly occurred more than 2500 years ago. In some
 357 deforested places in the Hyrcanian area, some woody species form scrub
 358 vegetation with plants such as *Paliurus spina-christi*, *Punica granatum*,
 359 *Crataegus* spp., *Berberis* spp.

361 From the middle of the 20th century, attention was given to the
 362 restoration of some of these forests (particularly lowland and submountain
 363 forests). Therefore, in many places, large-scale cultivation of *Alnus*
 364 *subcordata*, *Populus caspica*, *Acer* spp., *Populus* spp. and *Salix* spp. was
 365 conducted by many national organisations in Iran. Plantations of many non-
 366 native species, such as *Pinus*, *Cedrus* and other needle-leave trees (e.g.
 367 *Cupressus* and *Juniperus* species), were also created by these governmental
 368 departments. The latter trees were cultivated in some parts of Hyrcanian
 369 forests even in the natural forest communities. Many new or old introduced
 370 plant species have also been recorded in recent years in Iran especially in the
 371 north (e.g. [Mozaffarian, 1994](#); [Kukkonen et al., 2001](#); [Amini-Rad and](#)
 372 [Naqinezhad, 2003](#); [Naqinezhad and Saeidi Mehrvarz, 2007](#); [Naqinezhad et](#)
 373 [al., 2007](#); [Naqinezhad and Sharafi, 2007](#); [Hamzeh'ee and Naqinezhad, 2009](#)).
 374 Most of these species have their origins far away from Iran mainly South
 375 America or Africa. It is not exactly known when and how these species arrived
 376 in the north of Iran, but one possibility would be by migratory birds that visit for
 377 wintering in the northern wetlands of Iran. Although *Salvinia* is a native fern
 378 species, *Azolla*, another fern, has been introduced to contained pools from the
 379 Philippines. The fishery officers in Anzali observed no *Azolla* in 1990, but by
 380 1992 it had escaped and was dispersed in the wetland. The massive invasion
 381 by the latter fern has had catastrophic effects on natural plant and animal life
 382 of the Anzali wetland. It causes a similar situation in some parts of the
 383 Amirkola wetland. In hot years, with increasing water levels, the negative
 384 effect of *Azolla* is especially obvious.

385 Due to falling levels of the CS in the late 1960s, a rapid expansion of
 386 the *Phragmites* reed beds began and by the early 1980s large parts of the
 387 main wetland were covered. The recent rapid rise in water level in the wetland
 388 from early-80s to mid-90s stopped this expansion of *Phragmites* and even
 389 replaced many reed beds by open water areas ([Kazanci et al., 2004](#);
 390 [Ramezanpoor, 2004](#); [Anonymous, 2006](#)).

391 2.4 Past investigations

392 [Kazanci et al. \(2004\)](#) have studied the geomorphology of the lagoon of
 393 Anzali and surroundings in order to identify a series of natural cycles in the
 394 changes of the CS levels. These authors presented a series of maps of the
 395 extensive changes in the area of the lagoon since AD 1972 based on
 396 historical documents. The main results showed that, during sea level rise, the

397 lagoon area extends overall, but especially to the east, through flooding by the
398 sea. Five surface samples were studied for their pollen and dinocyst content.

399 [Lahijani et al. \(2009\)](#) have focused on the central Guilan and east
400 Mazandaran coasts, which are two accumulative areas, for disentangling
401 records of Late Holocene CS level change. The internal structure of the old
402 beaches in the Amirkola and Kiashahr areas was retrieved through ground
403 penetrating radar and showed prograding beaches. Their specifications are
404 similar of those in modern beaches in the area. In the Anzali spit, steep slope
405 seaward dipping layers with coarse-grained materials represent a high-energy
406 coast formed during early and the middle parts of last millennium.

407 The vegetation history of the area is poorly known from previous pollen
408 diagrams, although three records cover the last millennia. Recently, a pollen
409 diagram from the mire of Muzidarbon near Nowshahr at 550 m altitude
410 ([Ramezani et al., 2008](#)) has been published, covering the last 1000 years
411 (Fig. 1). It suggests a possible record of the Medieval Climatic Optimum and
412 the Little Ice Age (LIA). A clear increase of human activity is seen since the
413 beginning of the 19th century. The LIA is also definitely recorded by higher
414 lake levels most probably due to both lower summer temperatures leading to
415 reduced evaporation and higher annual precipitations in the Lake Almalou
416 sequence, on the eastern flanks of the Sahand Volcanic Complex in NW Iran
417 ([Djamali et al., 2009b](#)) (Fig. 1). The relatively long period of stability under the
418 Safavids (AD 1491–1736) resulted in prosperity, construction and the
419 development of much of Iran, but in the Almalou sequence it is not translated
420 by agriculture expansion but by nomadism, perhaps due to conflicts with
421 Ottoman Turks. In contrast, the modern period (AD 1850 onwards) is
422 characterized by expansion of agricultural activities to upland areas and
423 intensified pastoralism. A palynological study of the last 200 years was
424 obtained from a core in the NW of the Kara-Bogaz Gol, where human
425 activities were by far the strongest signal in the proxies ([Leroy et al., 2006](#)).
426 [Leroy et al. \(2007\)](#) published the results of a joint pollen and dinocyst study of
427 marine cores, one of them from the south basin of the CS, which covers the
428 period ca 5.5–0.8 cal. ka BP (core CP14, Fig. 1). Two phases with a stronger
429 river influence were identified: one from the core base to 3.9 cal. ka BP and
430 one from 2.1 to 1.7 cal. ka BP.

431 The study in the Turali barrier (Dagestan, Russia), although without
432 palynological investigations, is relevant as it has recorded two Caspian level
433 high stands, one 2600 years ago and one during the LIA ([Kroonenberg et al.,
434 2007](#)) (Fig. 1). High sea levels were also reconstructed from AD1300 to the
435 middle of the 19th century, i.e. the LIA, derived from radiocarbon dating of
436 several bays and lagoons on east coast of the CS ([Karpychev, 1993, 2001](#)).

437 The instrumental record going back to AD1837 shows a very stable CS
438 level until AD1935 followed by a drop of 2.7 m until AD1977 and a sudden
439 increase with a maximum high-stand in AD1995. These large variations have
440 been studied by several researchers, e.g. Arpe et al. (2000). Before the
441 instrumental records, scattered observations by travellers in the area are
442 available. Brückner (1890) collated some of them, such as islands emerging
443 from the sea in paintings or descriptions and markings left on walls along the
444 coast. Both can be used to extend the time span of CS level records though
445 with higher uncertainty because of the gaps in this document-based record.

446 A synthesis of various proxy records over the last 1000 years from the CS

447 to southern Mongolian Plateau indicates that the LIA in the arid central Asia
 448 was not only relatively wet (high P/E) but also had high precipitation (Chen et
 449 al., 2010). They suggest that cold temperatures during LIA would cause a
 450 southward shift of the westerly jet stream as the meridional temperature
 451 gradient increased, resulting in increased occurrences of mid-latitude cyclone
 452 activity and extreme events of precipitation.

453 3. Methods

454 3.1 Vegetation maps

455 For Amirkola, a detailed vegetation map at the plant community level
 456 has already been published in a local Persian journal by Asri and Moradi
 457 (2006). For the vegetation map used here in figures 2 and 3, many additional
 458 sources were however combined (Aghustin Sandar, 1969; Ghahreman et al.,
 459 2004). Many plant communities and their locations especially for the
 460 vegetation zones between the wetland and the sea are from Aghustin Sandar
 461 (1969). From 1969 up to now a clear alteration in these vegetation zones
 462 occurred and many of them do not exist anymore. One of the main reasons
 463 for this is the fluctuation of sea level. For the whole of Anzali wetland, no
 464 comprehensive vegetation map is available. The present map has been
 465 prepared by using personal assessments (satellite and aerial photos) and also
 466 data from Eftekhari (1995), Asri and Eftekhari (2002), Ghahreman and Attar
 467 (2003), Riazi (1996) and many unpublished data.

468 3.2 Coring and surface sampling

469 During field campaigns organised by the Iranian National Centre of
 470 Oceanography (INCO) in 2004, a series of cores were taken in the two
 471 lagoons. In Amirkola, four c. 1 m-long cores were collected with a Russian-
 472 type peat-coring device from the lagoon for sedimentological and
 473 palynological studies, of which three have been studied (Table 1). In Anzali,
 474 three cores (up to 2 m long) have been taken using a small heavy Kayak
 475 corer (Table 1). The core samples were preserved in wrapped PVC pipe with
 476 a 5.5 cm inner diameter. The cores were then transferred to the central
 477 laboratories of INCO for further studies. Subsampling took place immediately
 478 as no cooling facilities were available.

479 Moss pollsters and in some cases forest litters were taken in spring
 480 2006 from seven localities in the surroundings of Amirkola Lagoon in order to
 481 establish the modern pollen rain. Samples R1 to R4 correspond to four
 482 phytosociological surveys made by one of the authors in the *Alnus glutinosa*
 483 subsp. *barbata* forest to the south-west of the wetland (Table 2). The relevés
 484 were allocated according to Braun-Blanquet approach (Braun-Blanquet,
 485 1964). Samples a1 to a3 are as follows: a1: between alderwood and Amirkola
 486 Lagoon on an old tree bark of *Alnus glutinosa* subsp. *barbata* (Titiprizad
 487 Village), 30/03/2006; a2: Hassanbakande Village, 2 km to the CS, on the bark
 488 of an old *Salix alba* tree beside the lagoon, 03/04/2006; and a3:
 489 Hassanbakande Village, beside the lagoon under a *Phragmites* stand,
 490 03/04/2006.

491 3.3 Sedimentology

492 For both sites, dried samples were homogenized and a representative
 493 subsample was taken for grain size analysis. The distribution for the fraction
 494 coarser than 1 mm was determined using the standard wet sieving procedure.
 495 Grain-size analysis for particles less than 1 mm was undertaken using a
 496 “Fritsch Analysette Comfort 22” Laser Particle Sizer. Organic matter was
 497 determined by wet digestion through oxidation in hydrogen peroxide on bulk
 498 samples (Schumacher, 2002). The calcium carbonate was determined by
 499 using a Bernard calcimetre. The Laser particle size analysis of core HCGL02
 500 from Amirkola was done in France on a LS 13 320 Multi-Wavelength Particle
 501 Size Analyzer, ASTM standard calibrated.

502 The magnetic susceptibility was measured on core HCGL02 using a
 503 Bartington Multisusceptibility MS2E1 sensor in Laboratory of
 504 Palaeomagnetism of CEREGE, Aix-en-Provence, France. For Anzali core
 505 HCGA05, the same device was used at Brunel University to measure the
 506 magnetic susceptibility of the sediments. The measurements were made on
 507 dry sediment samples with the MS2B Dual Frequency Sensor. Three
 508 measurements were taken for each sample and then corrected for their
 509 sample volume as susceptibility values assume a sample volume of 10 cm³. A
 510 mean reading of the three calibrated measurements of magnetic susceptibility
 511 was then determined (Hamilton et al., 1986).

512 3.4 Chronology

513 For the Amirkola cores, two radiocarbon dates can be taken in
 514 consideration. The wood samples and shells were calibrated using
 515 respectively intcal04.14C and marine04.14C softwares (Hughen et al., 2004;
 516 Reimer et al., 2004).

517 An age-depth model for an Anzali core, core HCGA05, was obtained
 518 through ²¹⁰Pb dating on the top 50 cm (Vahabi-Asil, 2006; Lahijani et al.,
 519 2009). ²¹⁰Pb activities were measured by partial digestion of sediment
 520 samples using HNO₃ and HCl acids to extract grand-daughter ²¹⁰Po, which
 521 was then analysed by alpha spectrometry system using surface barrier
 522 detectors. The supported ²¹⁰Pb were estimated by assaying ²²⁶Ra through
 523 gamma spectrometry using HPGe detectors.

524 3.5 Palynology

525 For the Amirkola core HCGL02, seventeen samples of 1 cm³ were
 526 treated using the classical method of Moore et al. (1991): HCl at 10 %, HF,
 527 concentrated HCl, acetolysis and sieving at 160 µm. The seven surface
 528 samples were also treated with the same technique as described above. In a
 529 further study of the core residues, the thecamoebians and the foraminifera
 530 were counted on twenty-two samples that were additionally sieved at 10 µm.
 531 For the Anzali core HCGA05, twenty-seven samples taken every 6 cm were
 532 used for all the pollen, spores and dinocyst analyses. Initial processing of
 533 samples (1 ml in volume) involved the addition of sodium pyrophosphate to
 534 deflocculate the sediment. Samples were then treated with cold hydrochloric
 535 acid (10%) and cold hydrofluoric acid (32%), followed by a repeat HCl. The
 536 residual organic fraction was then screened through 120 and 10 µm mesh
 537 sieves and mounted on slides in glycerol. For both studies, the number of

538 pollen and spores counted was usually around 350. *Lycopodium* tablets were
 539 added at the beginning of the process for concentration estimates in the core
 540 samples only.

541 Incertae sedis 5b and some other palynomorphs typical of the Caspian
 542 Sea and the Kara-Bogaz Gol are illustrated in Leroy (in press). The taxonomy
 543 of many dinocyst taxa of the CS has been established by Marret et al. (2004).

544 Pollen percentages were calculated on the terrestrial sum (excluding
 545 aquatic, spores and unknown or unidentifiable pollen). The diagrams were
 546 plotted with psimpoll4 (Bennett, 2007). A zonation by cluster analysis
 547 (CONISS) after square root transformation was applied; that method is also
 548 available in psimpoll. The zonation, based only on terrestrial taxa, was
 549 calculated for the percentage diagrams.

550 The dinocysts were counted at the same time as pollen and other
 551 microfossils in Anzali. The foraminifera, the thecamoebians and the dinocysts
 552 were counted separately from the initial pollen count in Amirkola. The zones
 553 built on percentages of dinocysts are called dinozones. The total sum for
 554 percentage calculations (between 59 and 437) is made of all dinocysts except
 555 *Brigantedinium* spp. (including all round-brown specimens), because of its
 556 ubiquitous character and frequent dominance of the spectra. *Brigantedinium*
 557 is expressed as a percentage of the same sum as the other dinocysts.
 558 *Brigantedinium* is however included in the concentration diagram (in number
 559 of cysts per ml of wet sediment). In Amirkola, the zonation is visually defined
 560 based on the concentration curves of the thecamoebians, foraminifera and
 561 dinocysts whereas it is done on percentages by CONISS in Anzali. A ratio
 562 pollen concentration on dinocyst concentration (P:D) has been calculated
 563 according to McCarthy and Mudie (1998) to establish the terrestrial influence
 564 versus the marine one.

565 4. Results

566 4.1 Vegetation maps

567 4.1.1 Amirkola vegetation

568 In an investigation on this wetland and surrounding areas, 320 vascular
 569 plant species were found. About 105 species grow within or just beside the
 570 wetland. Twenty-seven species are submerged and floating and others are
 571 linked to wet places around the wetland (Ghahreman et al., 2004). Moreover,
 572 fifteen plant communities from three phytosociological classes were
 573 recognized within the lagoon and its surrounding (Asri and Moradi, 2006).

574 These communities are:

575 *Chara vulgaris*-*Chara canescentis* comm., *Nitella* sp. comm., *Potamogeton pectinatus*
 576 comm., *Ceratophyllum demersum* comm., *Ceratophyllum demersum*-*Azolla filiculoides*
 577 comm., *Nymphaea alba* comm., *Nelumbium nuciferum* comm., *Phragmites australis*
 578 comm., *Hydrocotyle ranunculoides* comm., *Typha latifolia* comm., *Cladium mariscus*
 579 comm., *Sparganium neglectum* comm., *Cyperus odoratus* subsp. *transcaucasus*
 580 comm., *Paspalum distichum* comm., and *Carex distans* comm..

581 Floristically, all these plant communities can be grouped into three main
 582 groups of vegetation: a peripheral large group including hygrophytic
 583 communities (vegetation zone 1) and helophytic communities (vegetation
 584 zone 2) and a central group including the real aquatic (hydrophytic)
 585 communities (vegetation zone 3) (Fig. 2) (Table 3).

586 Marginal (emergent) plants: The marginal parts of Amirkola wetland possess a high
 587 biodiversity of plant species which can be classified into two groups of vegetation:
 588 hygrophytic group (vegetation zone 1) which is less adapted to water-logged conditions
 589 and prefers drier habitats and the helophytic group (vegetation zone 2) with a higher
 590 adaptation to water. Some of the most important emergent plants of the marginal parts
 591 of the wetland are presented in Table 3.

592 Woody vegetation around the lagoon: Two main species, i.e. *Alnus glutinosa* subsp.
 593 *barbata* and *Salix alba*, dominate the closed forest around the lagoon. *Alnus glutinosa*
 594 subsp. *barbata* forms very dense stands in the western and south-western parts of the
 595 wetland with a surface area exceeding 100 ha. *Alnus glutinosa* subsp. *barbata*, an
 596 Euxino-Hyrcanian species, grows in the Hyrcanian lowland forests. *A. glutinosa* is a
 597 hygrophytic species, which forms some communities with other hygrophytic plants in
 598 lowland areas (Hamzeh'ee et al., 2008; Naqinezhad et al., 2008). The *Alnus* stands in
 599 the Amirkola wetland were considered as a plant association, *Galio elongatae–Alnetum*
 600 *barbatae* (Hamzeh' ee et al., 2008). Some characteristic herbal species of this
 601 community include *Thelypteris limbosperma*, *Galium elongatum*, *Phytolacca americana*
 602 and *Polygonum barbatum*. Other important species in this community are as following:
 603 *Smilax excelsa*, *Ficus carica*, *Berula angustifolia*, *Ranunculus lingua*, *Solanum*
 604 *persicum*, *Sambucus ebulus*, *Rubus sanctus*, *Lycopus europaeus*, *Carex riparia*,
 605 *Hydrocotyle vulgaris*, *Sparganium neglectum*, *Iris pseudacorus*, *Phragmites australis*,
 606 *Prunus divaricata*, *Mentha aquatica*, *Lythrum salicaria* and *Calystegia sylvestris*. *Alnus*
 607 *glutinosa* stands of Amirkola wetland constitute an intermediate and transitional
 608 vegetation community between the lagoonal system and the Hyrcanian closed lowland
 609 forests (e.g. Naqinezhad et al., 2008).

610 Central part, i.e. the open water area (vegetation zone 3): The flora of this part of the
 611 lagoon can be divided into submerged and floating plants (Table 3)..

612 4.1.2 Anzali wetland vegetation

613 The wetland is bordered to the north by sand dunes with grassland and
 614 scrubby vegetation and to the south by cultivated land (mainly ricefields) and
 615 patches of woodland (Fig. 3). The dominant vegetation throughout much of
 616 the Anzali wetland consists of vast beds of *Phragmites australis*.

617 In total, 291 plant taxa and 32 plant communities were recognized in
 618 the Anzali wetland (Asri and Eftekhari, 2002; Ghahreman and Attar, 2003).
 619 Details of the extent of 32 plant communities are given in Table 4. These plant
 620 communities are from the Siah-Keshim part of Anzali wetland (Fig. 3). Aquatic
 621 communities in Anzali wetland, like other wetland ecosystems, are
 622 homogenous, species-poor, mostly dominated by one or two species. Some
 623 plant communities like *Hydrocotyle ranunculoides* comm., *Nelumbium*
 624 *nuciferum* comm., *Paspalum distichum* comm. and *Phragmites australis*
 625 comm. possessing large masses, are observed in many parts of the wetland.

626 The pattern of vegetation zonation in the Anzali wetland is almost similar
 627 to that of Amirkola. Three main vegetation groups occur across all parts of the
 628 Anzali wetland (Fig. 3). These vegetation groups are ecologically adapted to
 629 different levels of groundwater.

630 Wet places surrounding the Anzali Lagoon (vegetation zone 1): Some plant species are
 631 adapted to relatively low humidity and grow on wet places near the wetland, rivers and
 632 on vast alluvial plains related to the wetland. This habitat is affected by flooding in
 633 heavy rain situations. Most parts of wetland margin are converted to cultivated lands
 634 now, but our evidence shows that many natural forest communities such as *Alnus*
 635 *glutinosa* subsp. *barbata* community, *Populus caspica* community, and *Alnus–Populus*
 636 community occurred as large pure patches in the area. Now only some sporadical and
 637 small stands of *Alnus glutinosa* subsp. *barbata*, *Populus caspica*, *Punica granatum*,
 638 *Gleditsia caspica*, *Salix alba*, *Celtis australis* and *Ulmus minor* occur in the area. No
 639 community is related to a dominant arboreal species. Some parts of this habitat
 640 (vegetation zone 1) have been covered with more or less large patches of *Juncus*
 641 *acutus* populations. The most important wetland plant growing in this zone are shown
 642 in table 3.

643 Marginal parts (vegetation zone 2): The next vegetation zone of the wetland occurs
 644 close to open water areas and is characterized by emergent helophytic flora and plant
 645 communities. This part constitutes the main vegetation cover in the wetland (Table 3).
 646 Central part, i.e. the open water area (vegetation zone 3): Although most parts of this
 647 zone particularly in the deepest places are occupied by open water areas without any
 648 vegetation cover, submerged and floating plant communities characterize the
 649 vegetation zone of this part (Table 3).

650 4.2 Lithology/sedimentology

651 Amirkola

652 The Amirkola cores generally consist of dark grey to yellowish silt and
 653 clay with horizons of sands and organic materials. The sandy layers contain
 654 articulated bivalves mostly of *Cerastoderma lamarcki*, *Didacna*, *Dreissena s.*
 655 *str.* and *Theodoxus pallasi*. Also frequently interspersed are plant remains,
 656 *Phragmites* and gastropods (Fig. 5 and 6). The content of organic matter
 657 increases from the base to the core tops. The calcium carbonate content
 658 shows an overall ascending trend along the cores with however a maximum
 659 reached earlier than the maxima of organic matter.

660 More especially, the lithology of core HCGL02 is from bottom to top:

661 98-81 cm: dark grey fine sands with fine dispersed plant remains.

662 81-70 cm: grey clay

663 70-55 cm: brown clay with very scattered *Phragmites* remains

664 55-44 cm: grey clay with gastropod fragments and *Phragmites* remains

665 44-29 cm: gastropod-rich silty mud with scattered fragments of *Phragmites*

666 29-25 cm: dark grey silty peat with *Phragmites* remains

667 25-0 cm: *Phragmites* peat.

668 This core is distinctively different from the two other cores with its very high
 669 content of organic matter in the top third of the core, probably due to its closer
 670 proximity to the shores. The magnetic susceptibility of core HCGL02 shows
 671 two peaks, the second one clearly in line with the brown clay.

672

673 Anzali

674 The visual characteristics and the sedimentology of the Anzali cores
 675 demonstrate the presence of a fine-grained dark grey sediment (Fig. 5 and 6).
 676 The amount of organic material varies along the cores without significant
 677 trend. Carbonate content has a background of 5% and a maximum of 25%.
 678 Silt and clay are the dominating fractions of the Anzali sediment. Sand-
 679 bearing layers appear in disconnected horizon along the cores.

680 More especially, for Anzali core HCGA05, the visual description is the
 681 following. The basal 20 cm contains a series of dark and grey muddy
 682 sediment: it has the highest contents of organic matter, carbonates and sand.
 683 Besides this, the physical properties of the sediment vary little. At around 100
 684 and 40 cm depth, two layers of organic-rich material occur. Discrete
 685 occurrences of sand occur only up to 64 cm depth. The top 25 cm consists of
 686 grey and light brown fine-grained material. The magnetic susceptibility is
 687 relatively stable, with slightly higher values at 138-130 cm depth.

688 4.3 Chronology

689 For the Amirkola cores, two ^{14}C dates provide us with a reasonably
 690 good estimation of the sedimentation rates in the eastern part of the western
 691 lobe of the lagoon despite the plateaux due to the young ages. For HCGL02,

692 the calibrated age of a wood fragment gave an age of AD1750 at 63-62 cm
 693 depth (Table 5). Therefore the base of the core could be extrapolated at AD
 694 1620 with a sedimentation rate of 0.25 cm per year. For core HCGL04 (Table
 695 5), a calibration could not be obtained using marine04.14C due to the too
 696 young age of the shells. In such young sequences, dating shells is more
 697 problematic than wood due to the existence of a reservoir effect and the
 698 uncertainty regarding which one to use, that of marine04.14C (Hughen et al.,
 699 2004) or another one. Indeed in the literature, various reservoir effects for the
 700 CS may be found to correct radiocarbon dates. They range from 290 to 440 yr
 701 with: 383 yr in Leroy et al. (2007), 290 yr in Kroonenberg et al. (2007), 390-
 702 440 yr in Kuzmin et al. (2007), and 345 to 384 yr in Karpychev (1993).

703 In the Anzali core HCGA05, the sedimentation rate is estimated as 0.5
 704 cm yr⁻¹ by using the CIC model based on experimental results. The total error
 705 in estimating unsupported ²¹⁰Pb is in the range of 8-19%. This sedimentation
 706 rate result is within the range of 0.1-0.6 cm yr⁻¹ determined by independent
 707 studies on sedimentation rate in Anzali Lagoon also using radionuclids (JICA,
 708 2004; Ardebili, 2005). Therefore the base of core HCGA05 is estimated at AD
 709 1670.

710 4.4 Palynology

711 Amirkola

712 Overall the pollen diagram from Amirkola is largely dominated by
 713 *Alnus*, with a significant abundance of *Carpinus* and Poaceae (Fig. 7). Four
 714 pollen zones were identified. In pollen zone Am2-1, *Alnus* percentages reach
 715 a maximum of 72%, while *Carpinus*, *Fagus*, *Quercus*, *Parrotia persica*,
 716 *Pterocarya* and *Ulmus-Zelkova* display continuous curves. In the non-arboreal
 717 pollen, *Artemisia* and Poaceae are relatively abundant. Pollen zone Am2-2
 718 and 3 (70 to 53 cm) are characterised by very sharp fluctuations of *Alnus* with
 719 a decrease to 12%. The Amaranthaceae-Chenopodiaceae, Asteraceae,
 720 *Artemisia*, Caryophyllaceae, and Cyperaceae largely benefit from this. A
 721 range of anthropogenic indicators including *Cerealia*-t., *Centaurea* (*C.*
 722 *solstitialis*-type), *Juglans*, *Morus*, and probably *Polygonum aviculare*-type
 723 pollen and the undeterminable grains are showing a brief abundance. The
 724 concentration in pollen and spores is minimal. The microcharcoals, already
 725 present in the zone below, display extremely high values in line with the
 726 brownish colour of the sediment. Then in pollen zone Am2-4, the spectra are
 727 roughly similar to pollen zone Am2-1, although the Poaceae are slightly more
 728 abundant. Towards the top of this zone, *Cerealia*-t. is again frequent. In this
 729 zone the aquatic taxa are abundant, with at first *Zannichellia palustris* and
 730 *Potamogeton* and then *Nymphaea* and *Typha-Sparganium*. *Pediastrum* is
 731 frequent at first; it is then followed by *Botryococcus* and various spores.
 732 Charcoal values are very low.

733 Three zones were identified in the dinocyst record. In the first part of
 734 dinozone Am2-1 up to 83 cm depth, some dinocysts and foraminifera are
 735 present in low numbers and become very scarce in the second part of this
 736 zone (Fig. 7). The dinocysts reflect the modern assemblages of the CS
 737 (Marret et al., 2004). In dinozone Am2-2 from 50 cm depth upwards, the
 738 assemblages change with the foraminifera and dinocysts being replaced by
 739 thecamoebians.

740 The four modern samples taken in the alder forest of Amirkola (R1 to
 741 R4) are completely dominated by pollen of *Alnus* (Fig. 8) and provide an
 742 extremely local signal whereas the three others samples taken in surrounding
 743 landscapes with lower density of alder trees better reflect the regional
 744 vegetation. The alder forest samples are the closest to the assemblages of
 745 pollen zone Am2-1. Sample a2 taken on the bark of a willow tree shows high
 746 values of *Salix*, while sample a3 taken in the *Phragmites* belt contains a good
 747 range of aquatic taxa and NPPs. The recently introduced *Azolla* fern is
 748 illustrated both by microspores and by massulae with the typical glochidia
 749 (Leroy, 1992) in these modern spectra but not visible in the sedimentary
 750 sequences.

751
 752 Anzali

753 Overall, the AP part of this diagram is dominated by *Carpinus betulus*-
 754 t., with a good abundance of *Alnus*, *Fagus*, *Quercus*, *Parrotia persica*,
 755 *Pterocarya* and *Ulmus-Zelkova* (Fig. 9). Within the non-arboreal pollen,
 756 Poaceae and Cyperaceae are the most abundant. The anthropogenic
 757 influence can be observed with the presence of *Vitis*, *Juglans* and *Cerealia*-t.
 758 and with the occurrence of isolated pollen rains of *Olea*, *Diospyros*, *Cucumis*
 759 and *Secale*-t. This situation changes little throughout the diagram, if not with
 760 slightly higher Cyperaceae in An5-1 and more *Alnus* in An5-2. A relatively
 761 large diversity of aquatic taxa and spores is present. A few grains of *Ruppia*
 762 occur in An5-2. Regarding the NPPs, green algae, such as *Botryococcus*,
 763 *Pediastrum boryanum* and *Tetraedron* are very abundant in the first samples
 764 of zone An5-1. Their values then drop and remain low throughout An5-2.
 765 These algal remains are frequent to abundant in zone An5-3. Incertae sedis
 766 5b, *Pterosperma* and foraminifera indicate the influence of the CS and these
 767 microfossils are frequent in the middle and top part of zone An5-1, and in
 768 most of An5-2.

769 Dinozone An5-1 is a short zone characterised by a clear dominance of
 770 *Spiniferites cruciformis*, typical of slightly brackish waters (Leroy et al., 2007).
 771 In Dinozone An5-2, the cysts of *Impagidinium caspiense* and of
 772 *Lingulodinium machaerophorum* form B are dominant, showing assemblages
 773 closer to those of the open CS (Leroy et al., 2007; Marret et al., 2004).
 774 Dinozone An5-3 sees the return of *S. cruciformis*, this time with moderate
 775 values alongside *I. caspiense*.

776 5. Interpretation and discussion

777 5.1 Sediment sources and lagoon history under various sea levels

778 In general the present study, confirming previous studies, indicates that
 779 the spits formed during Holocene high stands (Kroonenberg et al., 2000;
 780 Lahijani et al., 2009) have their source of sediment in the river supply and
 781 littoral drift.

782 The Amirkola Lagoon without river inflow is mainly infilled by eroded
 783 rice fields and vegetation. However, in the past, the Amirkola Lagoon had free
 784 water exchange with the CS (Fig. 10). The presence of articulated brackish
 785 bivalves in the sediment cores proves this connection. The latter closed later
 786 due to fluvial supply of the old Sefidrud redistributed through littoral drift. A

787 likely evolution of the present lagoon, with no change in sea level, would be
 788 the closing up of its surface with vegetation and sediment containing
 789 increased organic matter content. However, if the sea level continues to rise,
 790 a renewed invasion by the sea can easily happen. For comparison, the Turali
 791 barrier formed during sea level rise after AD 1977.

792 The regional geological setting has determined a change in shoreline
 793 direction from N – S in west Guilan to W – E in the central Guilan (Fig. 10).
 794 The southward longshore current strength declines in the Anzali region, which
 795 causes a reduction in water energy and the settlement of sediment. This led
 796 to the formation of the Anzali spit (Lahijani et al., 2009). Sediment for littoral
 797 drift is supplied from western Guilan rivers (Lahijani et al., 2008). During
 798 historical highstands, the Anzali spit broke into barriers with inlets. Therefore
 799 the Anzali Lagoon could receive more brackish seawater. It provided condition
 800 for bivalves that are frequent in marine water such as *Cerastoderma lamarcki*
 801 (Lahijani et al., 2009). Moreover, rivers crossing the Anzali Lagoon and
 802 barriers could nourish the Anzali spit (Fig. 10). Nowadays, the low energy
 803 environment in Anzali Lagoon allows deposition of fine-grained materials. The
 804 supply of nutrients from natural and anthropogenic sources and the
 805 dominantly limnic situation provide better environment for lagoonal vegetation.
 806 The high amount of organic material in the core sediments reflects the
 807 eutrophic environment of the Anzali Lagoon. In the future under rising sea
 808 level, the spit would again break up into barrier islands.

809 5.2 Vegetation and vegetation history

810 Both the Amirkola and Anzali wetlands are characterized as "aquatic
 811 wetlands" contrary to "telmatic wetlands" according to classification of
 812 Wheeler and Proctor (2000). A more or less similar zonation pattern occurs in
 813 both wetlands which is also consistent with many freshwater wetlands
 814 vegetation zonation elsewhere (e.g. Mitsch and Gosselink, 2000). In both
 815 wetlands, three main vegetation zones with specific floristic composition and
 816 plant communities for each zone have been recognised from land to water. All
 817 these vegetation zones are ecologically adapted to different levels of ground
 818 water.

819 The water depth is higher in the Anzali wetland and thus open water area
 820 in this wetland is larger than in Amirkola. Many parts of the open water area in
 821 Anzali Lagoon have no vegetation, except the Siah-Keshim part that has
 822 accumulated large amounts of aquatic submerged and floating plants.

823 Floristically, most of the plant species are the same in the two wetlands,
 824 except a few plants such as *Trapa natans*, *Nymphoides peltatum*, *Vallisneria*
 825 *spiralis* (all from vegetation zone 3), *Centella asiatica* (vegetation zone 1)
 826 which occur only in the Anzali wetland, and *Ranunculus lingua* which only
 827 occurs in Amirkola. The most prominent distinguishing feature between the
 828 two wetlands is the occurrence of large patches of *Alnus glutinosa* around
 829 Amirkola (especially in its SW parts), which constitutes some plant
 830 communities together with other aquatic herbs (Hamzeh'ee et al., 2008; Asri
 831 and Moradi, 2006). Some parts of the Amirkola wetland are under desiccation
 832 because of high accumulation of aquatic herbs (especially penetration of
 833 plants from zone 2 to the centre of the wetland). One of these places is in SW
 834 of Amirkola, Mordab-e Hassan–Alideh, which is near to *Alnus glutinosa*
 835 patches.

836 Different hydrological regimes characterise these two wetlands, Amirkola
 837 is a closed wetland well separated from the sea; but Anzali has some river
 838 connection with the sea. From the point of view of vegetation and floristic
 839 aspects, no clear evidence of salty water intrusion appears in Anzali. This is
 840 however not the case in the palynomorph assemblages, which show clear
 841 brackish waters both in surface samples and in sediment cores ([Kazancı et.,](#)
 842 [2004](#)).

843 Overall, the Hyrcanian lowland and plain vegetation is rather well
 844 represented by its pollen rain in the two lagoons with taxa such as *Pterocarya*,
 845 *Zelkova* and *Parrotia*. In addition, the Amirkola sequence records spectra
 846 typical of a forested wetland of alder.

847 The pollen diagram of Amirkola starting at AD 1620 (Fig. 11) shows a
 848 dense alder forest (most certainly *Alnus glutinosa*), but less dense than those
 849 present nowadays along the lagoon (Fig. 2 and 8). This environment was
 850 regularly flooded by the sea, as indicated by the presence of dinocysts typical
 851 of the CS, until 83 cm depth, or AD 1670. The marine influence decreases
 852 until it stops at 50 cm depth, or c. AD 1800. It is followed by a brief period of
 853 slightly brackish waters as illustrated by *Z. palustris*. As soon as the water
 854 body became isolated from the sea, the anthropogenic activities locally
 855 intensified and impacted the lagoon area. People further increased the
 856 disturbance of the natural environment from 70 cm depth, or c. AD 1720, by
 857 deliberate fires most likely related to the subsequent development of rice
 858 paddies. Therefore both the ruderal species of *Artemisia annua*, and some of
 859 the long-distance transport species of steppic *Artemisia*, are possible. In the
 860 Golestan National Park (GNP on Fig. 1), the high percentages of *Artemisia*
 861 *annua* in some floristic relevés is due to the rapid colonization in destroyed
 862 habitats after several successive flood events; these translate into 20-40% of
 863 *Artemisia* pollen in the surface spectra ([Djamali et al., 2009a](#)). The sudden fall
 864 of *Alnus* pollen during the Am2-3 pollen zone most probably indicates a large-
 865 scale deforestation of the alder forest by humans. Many possible causes for
 866 fire are, in order of likelihood: exceptionally intense Foehn effect, competition
 867 between large landowners to get agricultural land from the forest, and the
 868 intensified boat construction and marine trade during the rule of Nadir Shah of
 869 Afsharid Dynasty AD 1722 – 1750. Abandonment of this human activity
 870 occurred at 50 cm, or c. AD 1800. In the immediate vicinity of the lagoon, the
 871 alder forest returned quickly. As the lagoon became shallower and more
 872 isolated from the sea, a range of freshwater aquatic plants developed. The
 873 recent human influence can be seen more discreetly than earlier in the form of
 874 progressively increasing Poaceae and re-occurrence of *Cerealia-t*, reflecting
 875 the rice paddies now present in the region.

876 The pollen diagram of Anzali starting at c. AD 1670 illustrates a stable
 877 vegetation surrounding a wetland with a good representation from vegetation
 878 zones beyond the wetland, such as along the lower slopes of the Alborz
 879 Mountains (Fig. 11). Human influence is rather weak but continuous. NPPs,
 880 dinocysts and to a lesser extent aquatic vegetation (*Ruppia*) illustrate a
 881 slightly brackish lagoon continually influenced by the CS. The salinity of the
 882 water has, however, fluctuated throughout time, with the highest values,
 883 closer to those of the CS, from 152 to 86 cm depth, i.e. from c. AD 1700 to c.
 884 1830. Although there is no record of the occurrence of *Ruppia* in the wetland
 885 now ([Asri and Eftekhari, 2002](#); [Ghahreman and Attar, 2003](#)), some evidence

886 indicates that *Ruppia* grows in coastal lagoons where they are affected by the
 887 tidal cycles of the CS. For example the situation in Boujagh National Park,
 888 Guilan Province, where water flows from the CS to an inland wet depression
 889 in parts of the coast cause the formation of temporary wetlands with brackish
 890 water with *Ruppia* growth (Naqinezhad et al., 2006). Although the vegetation
 891 surveys do not show the influence of the CS, the presence of dinoflagellates
 892 in the phytoplankton survey and the sulphate concentration confirm the
 893 influence of the CS respectively in the entrance channel and far into the
 894 lagoon (Ramezanpoor, 2004).

895 It is interesting to note that the grab samples, collected in AD 1995 at the
 896 time of highest lake level (Kazancı et al., 2004), have *Alnus* percentages of 43
 897 to 60 % and to compare these high values with those of the top sample of
 898 core HCGA05 at 11 cm depth or AD 1982, which is therefore older than the
 899 grab samples, and which has much lower percentages. The whole core never
 900 reaches values higher than 38 %. It is generally known that *Alnus glutinosa*
 901 penetrates as an invasive community in wetlands that are desiccating.
 902 According to ecological succession, the alderwood community is the next
 903 seral community after the open water community toward drier inland forest.
 904 Some investigations have been carried out both on the succession from open
 905 water to alderwoods of *Alnus glutinosa*, which is generally considered as a
 906 final successional stage, and also on the further succession towards more
 907 drier *Alnus-Ulmion* communities (e.g. McVean, 1956; Fremstad, 1983;
 908 Prieditis, 1997; Kollar, 2001). The result of Kazancı et al. (2004) could indicate
 909 that in the recent years a natural afforestation occurs due to the accumulation
 910 of aquatic plant litter (large mats of *Phragmites* and other marginal plants) and
 911 subsequent mineralization in the open water parts of Anzali wetland with
 912 penetration of *Alnus* in these parts (e.g. Prieditis, 1997; Naqinezhad et al.,
 913 2008).

914 Overall, the diagram of Muzidarbon, south of Nowshahr, has less
 915 *Fagus*, *Quercus*, *Parrotia*, *Ulmus-Zelkova*, *Amaranthaceae-Chenopodiaceae*,
 916 *Artemisia* and *Poaceae* than the two lagoonal diagrams, but more *Carpinus*,
 917 reflecting the vegetation directly around the mire (Ramezani et al., 2008). The
 918 modern spectra of Amirkola fall in the same category of a record dominated
 919 by local vegetation. Anzali being a relatively large and open lagoon is able to
 920 record both local and regional vegetation, whereas Amirkola, despite the
 921 obvious dominance of *Alnus*, a local tree species, is able nevertheless to
 922 record a range of vegetation communities. This reflects the capacity of larger
 923 water bodies, i.e. Anzali 160 km², versus much smaller ones, i.e. Muzidarbon,
 924 0.003 km², to capture pollen rain from a larger area. At 12.3 km², Amirkola is
 925 of intermediate size and behaviour. An additional factor for the higher diversity
 926 of community represented is the river input to Anzali, virtually absent from
 927 Amirkola and Muzidarbon. These two factors, size of the open water body and
 928 size of catchment, have long been recognised in the literature to increase the
 929 record of the regional vegetation rather than local one (e.g. Pennington, 1979;
 930 Jackson, 1990).

931 5.3 Climate and sea levels

932 The more marine phase of the Amirkola core, from core base to 50 cm
 933 depth and the more marine phase of the Anzali core between 152 and 86 cm

934 depth, seem to be largely synchronous, dating to before AD 1800 in one case
935 and AD1700-1830 in the other (Fig. 11).

936 This corresponds to the high water levels of the LIA and agrees with data
937 from Brückner (1890). It was found that the CS level was 3 m higher around
938 AD1800 than 1835 according to markings on a coastal wall in Baku; also the
939 Derwisch and Naphtha Islands (off Cheleken in Turkmenistan) were
940 separated from AD1809 to 1814 and united by AD1819. Further evidence for
941 a brief low CS level was found around AD1719 to 1730, which was followed
942 by a high level in the 1740s obvious from several islands that could be seen
943 before and later submerged. The Derwisch and Naphtha Islands were
944 separated by a 3.0 to 3.7 m deep channel that could be crossed by foot
945 around AD1720. Roughly one can say that the CS had a low level, similar to
946 the present one, with an increase around AD1730 by 3 m and stayed high
947 until 1809, i.e. considerably higher than now. After that, the CS level dropped
948 sharply by 3.5 m to a level similar to the present and remained nearly stable
949 for more than 100 years.

950 During the LIA, Kroonenberg et al. (2007) reconstructed high water
951 levels from the barrier of Turali (Dagestan), which agree with the findings by
952 Brückner (1890). They explained these higher sea levels by a decreased
953 evaporation over the CS and/or enhanced precipitation over the very large CS
954 basin, which they hypothesised correlated with a lower solar activity.

955 The recent high levels over the last 30 years are not visible in Amirkola
956 as the lagoon is now closed and too remote from the sea, whereas in Anzali
957 the last sample at 11 cm depth, or AD 1982, with a re-increase of *I.*
958 *caspienense*, could be a sign of the recent high levels.

959 In the high altitude peat of Lake Almalou, the LIA has also been
960 recorded by high water table caused by lower evaporation, lower summer
961 temperatures and/or higher annual precipitation (Djamali et al., 2009b). All
962 these records agree in reconstructing more rainfall and higher water levels
963 during the LIA. Similar to the CS, Lake Almalou also had a high stand during
964 the LIA. This suggests that the cause for the high level of the CS does not
965 stem from the Volga alone but caused by regional climatic factors.

966 6. Conclusions

967 The southern part of CS, particularly the SW corner, with its subtropical
968 and humid Mediterranean climate hosts very specific Hyrcanian vegetation.
969 This climate is an island of high precipitation in an otherwise belt of
970 continental dryland. The moisture is clearly brought to the area by winds
971 mainly from the CS.

972 Combined analysis of pollen grains for terrestrial and aquatic vegetation
973 reconstruction, NPPs for parameters linked to water, dinocysts for past
974 salinities and sedimentological analyses appear to be suitable to reconstruct
975 past climatic and hydrological (sea level) changes in these environments. In
976 this case of minor climatic fluctuations over the last few centuries, the
977 investigation of terrestrial vegetation alone would not suffice, as the signal is
978 subtle and susceptible to anthropogenic modification. Fortunately, the study of
979 the full range of palynomorphs offers a comprehensive multiproxy approach.

980 The site of Amirkola shows a recent (*ca* 18th century) and temporary
981 destruction of the alder coastal forests especially by fire. Our data indicate

982 that the wetland forest can potentially recover quickly, although not
 983 completely. After a high stand, the lagoon becomes increasingly isolated from
 984 the sea.

985 In Anzali, the regional terrestrial vegetation is rather stable, except that
 986 the water body becomes more or less open to the sea. Specifically, during the
 987 period from c. AD 1700 to 1830, a stronger marine influence is detected in
 988 agreement with observations reported by Brückner (1890).

989 In both lagoons, the period of the late LIA corresponds to high water
 990 levels and contacts with the CS. However the two lagoons reacted differently
 991 to sea level rise. The high sediment supply of the Sefidrud nourished the
 992 beaches east of the Sefidrud mouth on a long distance. This easily
 993 compensated for the coastal erosion of the Amirkola spit due to sea level rise.
 994 In the case of the Anzali spit that broke into barrier islands during the late LIA,
 995 the sediment supplied through littoral drift and medium-size rivers was
 996 possibly insufficient to exceed the rate of erosional processes. The last sea
 997 level rise of the end of 20th century also opened new inlets in the lagoons of
 998 the southeast CS such as the Miankaleh and Gomishan Lagoons, whereas
 999 the Anzali spit with its high-density population was partially protected by
 1000 engineering measures.

1001 Moreover, in Amirkola, changes in the river delta geomorphology could
 1002 also have had a strong influence on the lagoon evolution since the position of
 1003 the main branch of the Sefidrud changes over time. The Amirkola Lagoon
 1004 being in precarious equilibrium, it is not impossible to predict that under
 1005 continued sea level rise, the lagoon will be once again in contact with the CS.

1006 A comparison of these two lagoons of the south of the CS to other sites,
 1007 Lake Almalou and the Turali barrier, indicates that the LIA climate was
 1008 regionally cooler and wetter, possibly also with less evaporation leading to
 1009 higher levels in the CS and other water bodies of the NW continental Middle
 1010 East.

1011 Overall our observations fit with the idea, proposed earlier by some
 1012 authors for the Caspian Sea to explain the wide Quaternary sea level
 1013 variations of more than 160 m amplitude (Karpichev, 1993; Chalié et al.,
 1014 1997): higher sea levels during cooler periods and lower sea levels during
 1015 warmer periods.

1016 **Acknowledgements**

1017 The coring and the sedimentological analyses were funded by the Iranian
 1018 National Institute for Oceanography in the framework of a research project
 1019 entitled "Investigation of the Holocene sediment along the Iranian coast of
 1020 Caspian Sea: central Guilan". One of the Anzali cores was taken during the
 1021 ICRP project of "Pollution record due to Caspian sea level rise in coastal
 1022 lagoons of Guilan Province" that was supported by the Centre for International
 1023 Scientific Studies and Collaboration, Iran. The authors are grateful to A.
 1024 Sharifi (INIO, previously INCO) who helped during the coring campaign. The
 1025 radiocarbon date of core HCGL02 was funded by V. Andrieu (Europôle
 1026 Méditerranéen de l'Arbois, France) and that of core HCGA04 by Brunel
 1027 University. M. Turner (Brunel University) has kindly revised the English of the
 1028 manuscript.

1029 **References**

- 1030 Afshin, Y., 1994. Iranian Rivers. Iranian Ministry of Energy, Jamab, part 2.
 1031 Aghustin Sangar, V., 1969. Ecological study of Amirkelayeh lagoon and the
 1032 vegetation variation from the lagoon to Caspian Sea. MSc thesis.
 1033 University of Tehran. (Unpublished thesis).
 1034 Amini-Rad, M., Naqinezhad, A., 2003, *Cyperus dives*, a new record from Iran.
 1035 Rostaniha 4, 111– 112.
 1036 Anonymous, 2006. The Ramsar convention manual, a guide to the convention
 1037 on wetlands (Ramsar, Iran, 1971). 4th edition. Switzerland: Ramsar
 1038 Convention Bureau. www.ramsar.org/pdf/lib/lib_manual2006e.pdf, Last
 1039 accessed 28 August 2010.
 1040 Ardebili, L., 2005. Geochemical study of Anzali Lagoon sediments. M.Sc.
 1041 Thesis, Bu Ali Sina University, Hamedan.
 1042 Arpe, K., Bengtsson, L., Golitsyn, G.S., Mokhov, I.I., Semenov, V.A.,
 1043 Sporyshev, P.V., 2000. Connection between Caspian sea-level
 1044 variability and ENSO. *Geophys. Res. Lett.* 27, 2693–2696.
 1045 Arpe, K., Leroy, S.A.G., 2007. The Caspian Sea Level forced by the
 1046 atmospheric circulation, as observed and modelled. *Quaternary*
 1047 *International* 173/174, 144-152.
 1048 Asri, Y., Eftekhari, Z., 2002. Flora and vegetation of Siah-Keshim lagoon. *J.*
 1049 *Environ. Stud.* 28, 1-19 (in Persian with English summary).
 1050 Asri, Y., Moradi, A., 2006. Plant associations and phytosociological map of
 1051 Amirkelayeh protected area. *Pajouhesh and Sazandegi* 70, 54-64. [in
 1052 Persian]
 1053 Bennett, K., 2007. Documentation for Psimpoll and Pscomb. [http://](http://www.chrono.qub.ac.uk/psimpoll/psimpoll.html)
 1054 www.chrono.qub.ac.uk/psimpoll/psimpoll.html, last accessed on 31 Aug.
 1055 2010.
 1056 Bobeck, H., 1951. Die natürlichen Wälder und Gehölzfluren Irans. Bonn.
 1057 *geogr. Abh.* 8, Bonn.
 1058 Braun-Blanquet, J., 1964. *Pflanzensoziologie: Grundzüge der*
 1059 *Vegetationskunde.* 3. Aufl. Springer, Wien.
 1060 Brückner, E., 1890. Klima-Schwankungen seit 1700 nebst Bemerkungen über
 1061 die Klimaschwankungen der Diluvialzeit. *Geographische Abhandlungen*
 1062 edited by A. Penck, Wien und Olmütz. Band IV, Heft 2, 153-484.
 1063 Chalié, F., the Caspian Sea INSU-Dytec Program Members, 1997. The
 1064 glacial-post glacial transition in the southern Caspian Sea. *C.R. Acad.*
 1065 *Sci.* 324, 309-316.
 1066 Chen, F.-H., Chen, J.-H., Holmes, J., Boomer, I., Austin, P., Gates, J.B.,
 1067 Wang, N.-L., Brooks, S.J., Zhang, J.-W., 2010. Moisture changes over
 1068 the last millennium in arid central Asia: a review, synthesis and
 1069 comparison with monsoon region. *Quat. Sc.Rev.* 29, 7-8, 1055-1068.
 1070 Djamali, M., de Beaulieu, J.-L., Campagne, P., Akhiani, H., Andrieu-Ponel, V.,
 1071 Ponel, P., Leroy, S., 2009a. Modern pollen rain-vegetation relationships
 1072 along a forest-steppe transect in the Golestan National Park, N-E Iran.
 1073 *Rev. Palaeobot. Palynol.* 153, 272-281.
 1074 Djamali, M., de Beaulieu, J.-L., Miller, N., Andrieu-Ponel, V., Berberian, M.,
 1075 Gandouin, E., Lahijani, H., Ponel, P., Salimian, M., Guiter, F., 2009b. A
 1076 late Holocene pollen record from Lake Almalou in NW Iran: evidence for

- 1077 changing land-use in relation to some historical events during the last
1078 3700 years. *J. Archaeol. Sc.* 36, 1364-1375.
- 1079 Djazirei, M.H., 1965. Contribution à l'étude des forêts primaires de la
1080 Caspienne. *Bull. Inst. Agron. Gembloux* 33, 1, 36-71.
- 1081 Eftekhari, T., 1995. Vegetation mapping of Siah-Keshim lagoon (Anzali
1082 wetland). MSc thesis. University of Tarbiat-Moallem (Unpublished
1083 thesis).
- 1084 Fremstad, E., 1983. Role of black alder (*Alnus glutinosa*) in vegetation
1085 dynamics in West Norway. *Nord. J. Bot.* 3,393–410.
- 1086 Frey, W., Probst, W., 1986. A synopsis of the vegetation of Iran, in:
1087 Kürschner, H. (ed.), Contribution of the vegetation of southwest Asia. Dr.
1088 Ludwig Reichert, Wiesbaden, pp. 1-43.
- 1089 Ghahreman, A., Attar, F., 2003. Anzali wetland in danger of death (an
1090 ecologic-floristic research) (special issue, Anzali lagoon). *Journal of*
1091 *Environmental Studies* 28, 1-38 [in Persian with English summary].
- 1092 Ghahreman, A., Naqinezhad, A.R., Attar, F., 2004. Habitats and flora of the
1093 Chamkhaleh-Jirbagh coastline and Amirkelayeh wetland. *Journal of*
1094 *Environmental Studies* 33, 46-67 (In Persian with English abstract).
- 1095 Hamilton, A.C., Magowan, W., Taylor, D., 1986. Use of the Bartington Meter
1096 to determine tile magnetic susceptibility of organic-rich sediments from
1097 western Uganda. *Phys. Earth Planet. Int.* 42, 5-9.
- 1098 Hamzeh'ee, B., Naqinezhad, A., 2009. *Arthraxon* P. Beauv. (Gramineae) and
1099 *Carex caryophyllea* (Cyperaceae), new genus and species records from
1100 Iran. *Iran. J. Bot.* 15, 1, 68-71.
- 1101 Hamzeh'ee, B., Naqinezhad, A., Attar, F., Ghahreman, A., Assadi, M.,
1102 Prieditis, N., 2008. Phytosociological survey of remnant *Alnus glutinosa*
1103 subsp. *barbata* communities in the lowland Caspian forest of northern
1104 Iran. *Phytocoenologia* 38, 117-132.
- 1105 Hughen, K.A., Baillie, M.G.L., Bard, E., Bayliss, A., Beck, J.W., Bertrand, C.,
1106 Blackwell, P.G., Buck, C.E., Burr, G., Cutler, K.B., Damon, P.E.,
1107 Edwards, R.L., Fairbanks, R.G., Friedrich, M., Guilderson, T.P., Kromer,
1108 B., McCormac, F.G., Manning, S., Bronk Ramsey, C., Reimer, P.J.,
1109 Reimer, R.W., Remmele, S., Southon, J.R., Stuiver, M., Talamo, S.,
1110 Taylor, F.W., van der Plicht, J., Weyhenmeyer, C.E., 2004. Marine04
1111 marine radiocarbon age calibration, 0-26 cal kyr BP. *Radiocarbon* 46,
1112 1059-1086.
- 1113 Jackson, S.T., 1990. Pollen source area and representation in small lakes of
1114 the northeastern United States. *Rev. Palaeobot. Palynol.* 63, 53-76.
- 1115 JICA, 2004. The study on integrated management for ecosystem conservation
1116 of the Anzali Wetland. Japan International Cooperation Agency (Nippon
1117 Koeco), Chiyoda-ku, Tokyo.
- 1118 Karpychev, Y.A., 1993. Reconstruction of Caspian Sea-level fluctuations:
1119 radiocarbon dating coastal and bottom deposits. *Radiocarbon* 35, 3,
1120 409–420.
- 1121 Karpychev, Y.A., 2001. Variations in the Caspian Sea level in the historic
1122 epoch. *Water Resources*, 28,1, 1-14.
- 1123 Kazancı, N., Gulbabazadeh, T., Leroy, S.A.G., Ileri, O., 2004. Sedimentary
1124 and environmental characteristics of the Gilan-Mazenderan plain,
1125 northern Iran: influence of long- and short-term Caspian water level

- 1126 fluctuations on geomorphology. *Journal of Marine Systems* 46, 1-4, 145-
1127 168.
- 1128 Khalili, A., 1973. Precipitation patterns of Central Elburz. *Theoretical and*
1129 *Applied Climatology* 21, 215–232.
- 1130 Klige, R.N., Selivanov, A.D., 1995. Budget of sedimentary material in the
1131 Caspian Sea and its possible role in water-level changes. *Water*
1132 *Resources* 22, 330–335.
- 1133 Kollar, J., 2001. The Borska Nizina lowland black alder forests and their
1134 ecological evaluation. *Ekologia* 20 (Suppl. 3), 202–207.
- 1135 Kousari, S., 1986. Evolution of Sefidrud Delta. *Development in Geological*
1136 *Education* 1, 51–62.
- 1137 Kousari, S., 1988. Evolution of Anzali lagoon. *Development in Geological*
1138 *Education* 12 and 13, 29–37.
- 1139 Krasnozhan, G.F., Lahijani, H., Voropayev, G.V., 1999. Sefidrud delta
1140 evolution from space images of the Caspian coast of Iran. *Earth*
1141 *Research from Space* 1, 105–111.
- 1142 Kroonenberg, S.B., Abdurakhmanov, G.M., Badyukova, E.N., van der Borg,
1143 K., Kalashnikov, A., Kasimov, N.S., Rychagov, G.I., Svitoch, A.A.,
1144 Vonhof, H.B., Wesselingh, F.P., 2007. Solar-forced 2600 BP and Little
1145 Ice Age highstands of the Caspian Sea. *Quaternary International*,
1146 173/174, 137-143.
- 1147 Kroonenberg, S.B., Badyukova, E.N., Storms, J.E.A., Ignatov, E.I., Kasimov,
1148 N.S., 2000. A full sea-level cycle in 65 years: barrier dynamics along
1149 Caspian shores. *Sedimentary Geology* 134, 257–274.
- 1150 Kukkonen, I., Ghahreman, A., Naqinezhad, A., 2001. *Isolepis cernua*
1151 (Cyperaceae) a new record from north of Iran. *Iran. J. Bot.* 9, 107-110.
- 1152 Kuzmin, Y.V., Nevesskaya, L.A., Krivonogov, S.K., Burr, G.S., 2007. Apparent
1153 ¹⁴C ages of the 'pre-bomb' shells and correction values (*R*, ΔR) for
1154 Caspian and Aral Seas (Central Asia). *Nuclear Instruments and Methods*
1155 *in Physics Research B* 259, 463-466.
- 1156 Lahijani, H., 1997. Riverine Sediments and Stability of Iranian Coast of the
1157 Caspian Sea. Ph.D. Thesis, Russian Academy of Sciences.
- 1158 Lahijani, H.A.K., Rahimpour-Bonab, H., Tavakoli, V., Hosseindoost, M., 2009.
1159 Evidence for late Holocene highstands in Central Guilan–East
1160 Mazanderan, South Caspian coast, Iran. *Quaternary International* 197,
1161 55–71.
- 1162 Lahijani, H.A.K., Tavakoli, V., Amini, A.H., 2008. South Caspian River Mouth
1163 Configuration Under Human Impact and Sea level Fluctuations.
1164 *Environmental Sciences* 5, 2, 65-86.
- 1165 Leroy, S.A.G., 1992. Palynological evidence of *Azolla nilotica* Dec. in Recent
1166 Holocene of eastern Nile Delta, and its environment. *Veget. Hist.*
1167 *Archaeobot.* 1, 43-52.
- 1168 Leroy, S.A.G., in press. Palaeoenvironmental and palaeoclimatic changes in
1169 the Caspian Sea region since the Lateglacial from palynological
1170 analyses of marine sediment cores. *Geography, Environment,*
1171 *Sustainability.* Faculty of Geography of Lomonosov Moscow State
1172 University and by the Institute of Geography of RAS.
- 1173 Leroy, S.A.G., Warny, S., Lahijani, H., Piovano, E.L., Fanetti, D., Berger, A.R.,
1174 2010. The role of geosciences in the mitigation of natural disasters: five
1175 case studies, in: Beer, T. (ed.), *Geophysical Hazards: Minimising risk,*

- 1176 maximising awareness. Springer Science, in series International Year of
1177 Planet Earth, pp. 115-147.
- 1178 Leroy, S.A.G., Marret, F., Gibert, E., Chalié, F., Reyss J-L., Arpe K., 2007.
1179 River inflow and salinity changes in the Caspian Sea during the last
1180 5500 years. *Quaternary Science Reviews* 26, 3359-3383.
- 1181 Leroy, S.A.G., Marret, F., Giralt, S., Bulatov, S.A., 2006. Natural and
1182 anthropogenic rapid changes in the Kara-Bogaz Gol over the last two
1183 centuries by palynological analyses. *Quaternary International* 150, 52-
1184 70.
- 1185 Leroy, S.A.G., Roiron, P., 1996. Final Pliocene macro and micro floras of the
1186 paleovalley of Bernasso (Escandorgue, France). *Rev. Palaeobot. Palynol.*
1187 94, 295-328.
- 1188 Malinin, V.N., 1994. Problems of the Caspian Sea-level Forecasting. Saint
1189 Petersburg PGGMI Publication.
- 1190 Marret, F., Leroy, S.A.G., Chalié, F., Gasse, F., 2004. New organic-walled
1191 dinoflagellate cysts from recent sediments of central Asian seas. *Review*
1192 *of Palaeobotany and Palynology* 129, 1–20.
- 1193 McCarthy, F.M.G., Mudie, P.J., 1998. Oceanic pollen transport and
1194 pollen:dinocyst ratios as markers of late Cenozoic sea level change and
1195 sediment transport. *Palaeogeography, Palaeoclimatology,*
1196 *Palaeoecology* 138, 187–206.
- 1197 McVean, D.N., 1956. Ecology of *Alnus glutinosa* (L.) Gaertn: V. notes on
1198 some British alder populations. *J. Ecol.* 44,321–330.
- 1199 Meusel, H., Jäger, E., Weinert, E., 1965. Vergleichende Chorologie der
1200 zentraleuropäische Flora. Band I. Gustav Fischer Verlag. Jena.
- 1201 Mikhailov, V.N., 1997. River mouths of Russia and adjacent countries. GEOC,
1202 Moscow [in Russian].
- 1203 Mitsch, W.J., Gosselink, J.G., 2000. Wetlands. John Wiley & Sons, New York.
- 1204 Moore, P.D., Webb, J.A., Collinson, M.E., 1991. Pollen Analysis, 2nd ed.
1205 Blackwell Scientific Publications, Oxford.
- 1206 Mozaffarian, V., 1994. Studies on the flora of Iran, new species and new
1207 records. *Iranian Journal of Botany* 6, 235–243
- 1208 Naqinezhad, A., Hamzeh'ee B., Attar, F. 2008. Vegetation – environment
1209 relationship in the Black alder forests of Caspian lowlands, N. Iran. *Flora*
1210 203, 567-577.
- 1211 Naqinezhad, A., Saeidi Mehrvarz, Sh., 2007. Some new records for Iran and
1212 Flora Iranica area collected from Boujagh National Park, N. Iran. *Iran. J.*
1213 *Bot.* 13, 112-119.
- 1214 Naqinezhad, A., Saeidi, Sh., Noroozi, M., Faridi, M., 2006. Contribution to the
1215 vascular and bryophyte flora as well as habitat diversity of the Boujagh
1216 National Park, N. Iran. *Rostaniha* 7, 83-106.
- 1217 Naqinezhad, A., Sharafi, M., 2007. Two new records from Gilan and
1218 Mazandaran provinces, N. Iran. *Iran. J. Bot.* 13, 95-98.
- 1219 Naqinezhad, A., Saeidi, Sh., Djavadi, B., Ramezankhah, S., 2007. A new
1220 genus record of Asteraceae (*Soliva pterosperma*) for the flora of Iran.
1221 *Iran. J. Bot.* 13, 104-106.
- 1222 Pennington, W., 1979. The origin of pollen in lake sediments: an enclosed
1223 lake compared with one receiving inflow streams. *The New Phytologist*
1224 83, 189–213.
- 1225 Pirazolli, P.A., 2000. Sea Level Changes, The Last 20,000 years. Wiley, New

- 1226 York.
- 1227 Prieditis, N., 1997. *Alnus glutinosa*-dominated wetland forests of the Baltic
1228 region: community structure, syntaxonomy and conservation. *Plant Ecol.*
1229 129, 49–94.
- 1230 Ramezani, E., Joosten, H., Mohadjer, M.R.M., Knapp, H.-D., Ahmadi, H.,
1231 2008. The late-Holocene vegetation history of the Central Caspian
1232 (Hyrcanian) forests of northern Iran. *The Holocene* 18, 2, 305–319.
- 1233 Ramezanpoor, Z., 2004. Ecological study of phytoplankton of the Anzali
1234 lagoon (N Iran) and its outflow into the Caspian Sea. *Czech Phycology,*
1235 *Olomouc* 4, 145-154.
- 1236 Reimer, P.J., Baillie, M.G.L., Bard, E., Bayliss, A., Beck, J.W., Bertrand, C.,
1237 Blackwell, P.G., Buck, C.E., Burr, G., Cutler, K.B., Damon, P.E.,
1238 Edwards, R.L., Fairbanks, R.G., Friedrich, M., Guilderson, T.P., Hughen,
1239 K.A., Kromer, B., McCormac, F.G., Manning, S., Bronk Ramsey, C.,
1240 Reimer, R.W., Remmele, S., Southon, J.R., Stuiver, M., Talamo, S.,
1241 Taylor, F.W., van der Plicht, J., Weyhenmeyer, C.E., 2004. IntCal04
1242 terrestrial radiocarbon age calibration, 0-26 cal kyr BP. *Radiocarbon* 46,
1243 1029-1058.
- 1244 Riazi, B., 1996. Siah-Keshim, the protected area of Anzali wetland.
1245 Department of Environment Publication, Tehran.
- 1246 Rodionov, S.N., 1994. Global and Regional Climate Interaction: The Caspian
1247 Sea Experience. *Water Science and Technology Library*, vol. 11. Kluwer
1248 Academic Press, Baton Rouge.
- 1249 Rudolf, B., Fuchs T., Schneider U., Meyer-Christoffer A., 2003. Introduction of
1250 the Global Precipitation Climatology Centre (GPCC), Deutscher
1251 Wetterdienst, Offenbach a.M.; pp. 16, available on request per email
1252 gpcc@dwd.de or by download from GPCC's Website.
- 1253 Rychagov, G.I., 1997. Holocene oscillations of the Caspian Sea and forecasts
1254 based on paleogeographical reconstructions. *Quaternary International*
1255 41/42, 167–172.
- 1256 Schumacher, B.A., 2002. Methods for the determination of total organic
1257 carbon (TOC) in soils and sediments. US Environmental Protection
1258 Agency, Las Vegas, NV.
- 1259 Terziev, S.F., 1992. *Hydrometeorology and Hydrochemistry of Seas*, Vol. 6
1260 the Caspian Sea, No 1. Hydrometeorological Conditions,
1261 Gidrometeoizdat, Leningrad [in Russian].
- 1262 Tregubov, V., Mobayen, S., 1970. Guide pour la carte de la végétation
1263 naturelle de l' Iran. 1:2500000. – Bull. 14, Project UNDP/FAO IRA 7.
- 1264 Uppala, S.M., Kållberg, P.W., Simmons, A.J., Andrae, U., da Costa Bechtold,
1265 V., Fiorino, M., Gibson, J.K., Haseler, J., Hernandez, A., Kelly, G.A., Li,
1266 X., Onogi, K., Saarinen, S., Sokka, N., Allan, R.P., Andersson, E., Arpe,
1267 K., Balmaseda, M.A., Beljaars, A.C.M., van de Berg, L., Bidlot, J.,
1268 Bormann, N., Caires, S., Chevallier, F., Dethof, A., Dragosavac, M.,
1269 Fisher, M., Fuentes, M., Hagemann, S., Hólm, E., Hoskins, B.J.,
1270 Isaksen, I., Janssen, P.A.E.M., Jenne, R., McNally, A.P., Mahfouf, J.-F.,
1271 Morcrette, J.-J., Rayner, N.A., Saunders, R.W., Simon, P., Sterl, A.,
1272 Trenberth, K.E., Untch, A., Vasiljevic, D., Viterbo, P., Woollen, J., 2005.
1273 The ERA-40 re-analysis, *Quart. J. R. Meteorol. Soc.* 131, 2961-3012.
- 1274 Vahabi-Asil, F., 2006. Dating Caspian Sea and Anzali Lagoon sediments
1275 using ²¹⁰Pb technique. M.Sc. Thesis, The University of Guilan, Rasht.

- 1276 Varushchenko, S.I., Varushchenko, A.N., Klige, R.K., 1987. Changes in the
1277 Regime of the Caspian Sea and Closed Basins in Time. Moscow, Nauka
1278 [in Russian]
- 1279 Warrick, R.A., 1993. Climate and sea level change, a synthesis, in: Warrick,
1280 R.A. (Ed.), Climate and Sea-level Change, Observations, Projections
1281 and Implications. Cambridge University Press, Cambridge, pp. 3–21.
- 1282 Wheeler, B.D., Proctor, M.C.F., 2000. Ecological gradients, subdivisions and
1283 terminology of north-west European mires. *J. Ecol.* 88, 187–203.
- 1284 Zenkovich, V.P., 1957. Structure of the South-east coast of the Caspian Sea,
1285 USSR Academy of Sciences. Oceanographic Commission Works II, 4–
1286 11.
- 1287 Zohary, M., 1973. Geobotanical foundations of the Middle East. 2 vols.
1288 Fischer Verlag, Stuttgart, Amsterdam.
1289

1290 **Tables**

1291 Table 1: List of core names, locations, lengths and depths. In bold, cores
1292 studied for palynology.

Site	Core name	Latitude N	Longitude E	Water depth in cm	Length in cm
Amirkola	HCGL02	37 21 25.6	50 11 42.2	100	95
	HCGL03	37 21 7.2	50 11 42.3	200	33
	HCGL04	37 20 33.1	50 11 33.4	200	80
Anzali	HCGA05	37 26 56.6	49 22 49.8	300	170
	HCGA04	37 27 06.7	49 23 35.7	300	164
	HCGA08 (= PLS08)	37 26 56	49 22 49	300	92

1293

1294

1295 Table 2: Phytosociological surveys 25 by 25 m around the moss pollsters and
1296 forest litter taken for modern pollen rain in the Amirkola wetland. The number
1297 opposite to each plant indicates its cover-abundance according to the Braun-
1298 Blanquet scale. DBH = diameter at breast height.

1299

1300

1301

1302

1303

1304

1305

1306

1307

1308

1309

1310

1311

1312

1313

1314

1315

1316

1317

1318

1319

1320

1321

1322

1323

1324

1325

1326

1327

1328

1329

1330

1331

1332

1333

1334

1335

Relevé number	R1	R2	R3	R4
Average DBH (in cm)	27	24	21	23
Number of trees	4	11	15	18
Associated species				
<i>Alnus glutinosa</i> subsp. <i>barbata</i>	3	4	5	5
<i>Berula angustifolia</i>			1	
<i>Calystegia sylvestris</i>		1	1	
<i>Carex riparia</i>	4	4	1	1
<i>Ficus carica</i>	2	2	1	1
<i>Galium elongatum</i>	1	1	1	1
<i>Hydrocotyle vulgaris</i>		2	1	1
<i>Iris pseudacorus</i>	1	1	2	1
<i>Lycopus europaeus</i>	1		1	
<i>Nasturtium officinale</i>				1
<i>Polygonum</i> sp.	1		1	1
<i>Prunus divaricata</i>				1
<i>Ranunculus lingua</i>				1
<i>Ranunculus scleratus</i>	2			
<i>Rubus caesius</i>	1		1	
<i>Rubus sanctus</i>	1	1	1	1
<i>Rumex sanguineus</i>			1	
<i>Sambucus ebulus</i>	1	1	1	
<i>Smilax excelsa</i>	2	1	1	1
<i>Solanum dulcamara</i>		1		1
<i>Thelypteris limbosperma</i>	1	2	2	2
<i>Urtica dioica</i>			1	

Species collected around the relevés

Sparganium neglectum, *Cladium mariscus* subsp. *mariscus*, *Rumex conglomeratus*, *Ulmus minor*, *Polygonum hydropiper* subsp. *hydropiper*, *Solanum nigrum*, *Sonchus oleraceus*, *Periploca graeca*, *Phragmites australis*, *Phytolacca americana*, *Cardamine hirsuta*, *Carex remota* subsp. *remota*, *Lythrum salicaria*, *Mentha aquatica*, *Geum urbanum*, *Humulus lupulus*, *Cornus australis*

1336 Table 3: List of the most important plants found in each vegetation zone in
 1337 Amirkola and Anzali wetlands. Underlined species are found exclusively in
 1338 Anzali. The species with asterisk are only found in Amirkola.
 1339

Vegetation zone 3	
Floating plants	Submerged plants
<i>Azolla filiculoides</i> , <i>Hydrocharis morsus-ranae</i> , <i>Lemna gibba</i> , <i>L. minor</i> , <i>Nymphaea alba</i> , <u><i>Nymphoides peltatum</i></u> , <i>Potamogeton natans</i> , <i>P. nodosus</i> , <i>Ricciaocarpus natans</i> * (aquatic liverwort), <i>Salvinia natans</i> , <i>Spirodella polyrhiza</i> , <i>Wolfia arhyza</i> .	<i>Batrachium trichophyllum</i> , <i>Callitriche palustris</i> , <i>Ceratophyllum demersum</i> , <i>Chara fragilis</i> (green algae), <i>Hydrilla verticillata</i> , <i>Lemna trisulca</i> , <i>Myriophyllum spicatum</i> , <i>Najas</i> spp., <i>Nitella</i> spp. (green algae), <i>Potamogeton crispus</i> , <i>P. lucense</i> , <i>P. pectinatus</i> , <i>P. pusilus</i> , <i>Riccia fluitans</i> * (aquatic liverwort), <i>Utricularia neglecta</i> , <u><i>Vallisneria spiralis</i></u> , <i>Zannichellia palustris</i> .
Vegetation zone 1	Vegetation zone 2
<i>Abutilon theophrasti</i> , <i>Alnus glutinosa</i> subsp. <i>barbata</i> , <i>Alisma plantago-aquatica</i> , <i>Bidens tripartita</i> , <i>Butomus umbellatus</i> , <u><i>Centella asiatica</i></u> , <i>Coix lacryma-jobi</i> , <i>Gleditsia caspica</i> , <i>Kosteletzkya pentacarpa</i> , <i>Inula britannica</i> , <i>Ludwigia palustris</i> , <i>Lythrum salicaria</i> , <i>Mentha aquatic</i> , <i>Ranunculus dolosus</i> , <i>R. scleratus</i> , <i>Sagittaria trifolia</i> , <i>Smilax excels</i> , <i>Rubus</i> spp., <u><i>Pterocarya fraxinifolia</i></u> , <u><i>Populus caspica</i></u> , <i>Polygonum</i> spp., <i>Salix</i> spp.	<i>Berula angustifolia</i> , <i>Cladium mariscus</i> , <i>Galium elongatum</i> , <i>Hydrocotyle ranunculoides</i> , <i>Iris pseudacorus</i> , <i>Nasturtium officinale</i> , <i>Nelumbium nuciferum</i> , <i>Phragmites australis</i> , <i>Pteridium aquilinum</i> , <i>R. lingua</i> *, <i>Schoenoplectus lacustris</i> , <i>Solanum dulcamara</i> , <i>Solanum persicum</i> , <i>Sparganium neglectum</i> , <i>Typha</i> spp.

1340

1341

1342

1343

1344

Table 4: Plant communities within three main vegetation zones in the Anzali wetland. The cover percentage for each community is estimated only in Siah-Keshim wetland (the southern lobe of the Anzali wetland).

Plant community	Some other characteristic or companion species	Approx. %
Vegetation zone #1		8.9
<i>Bidens tripartita</i> - <i>Polygonum hydropiper</i>	<i>Cyperus fuscus</i> , <i>Fimbristylis bisumbellata</i> , <i>Cyperus difformis</i>	5.5
<i>Paspalum distichum</i>		0.8
<i>Rorippa islandica</i>		0.4
<i>Cyperus serotina</i>		0.4
<i>Alisma plantago-aquatica</i> - <i>Sagittaria sagittifolia</i>		0.4
<i>Carex riparia</i>	<i>Berula angustifolia</i>	0.4
<i>Juncus effuses</i>	<i>Polygonum hydropiper</i>	0.4

<i>Cyperus longus</i>		0.4
<i>Bidens cernua</i>		0.2
Vegetation zone #2		51.1
<i>Phragmites australis</i>	<i>Solanum persicum, Azolla filiculoides, Sparganium erectum subsp. neglectus</i>	35.2
<i>Sparganium erectum var. neglectum</i>	<i>Berula angustifolia, Nasturtium officinalis</i>	13.2
<i>Typha latifolia</i>	<i>Phragmites australis, Paspalus distichum</i>	1
<i>Nelumbium nuciferum</i>		0.4
<i>Schoenoplectus lacustris</i>		0.4
<i>Hydrocotyle ranunculoides</i>		0.4
<i>Iris pseudacorus</i>		0.4
<i>Nasturtium officinalis</i>	<i>Alisma plantago-aquatica, Berula angustifolia</i>	0.1
Vegetation zone #3		15.8
<i>Trapa natans-Potamogeton crispus</i>	<i>Wolffia arrhiza, Zannichellia palustris, Azolla filiculoides</i>	11.1
<i>Lemna minor-Azolla filiculoides</i>	<i>Wolffia arrhiza, Lemna trisulca</i>	1.2
<i>Lemna minor-Spirodella polyrrhiza</i>	<i>Azolla filiculoides</i>	0.1
<i>Lemna minor-Lemna trisulca</i>	<i>Utricularia neglecta, Wolffia arrhiza</i>	0.1
<i>Salvinia natans</i>	<i>Azolla filiculoides, Spirodella polyrrhiza</i>	0.1
<i>Hydrocharis morsus-ranae</i>	<i>Utricularia neglecta</i>	0.1
<i>Utricularia neglecta</i>	<i>Lemna trisulca, Zannichellia palustris</i>	0.1
<i>Trapa natans-Potamogeton pectinatus</i>		2
<i>Potamogeton pectinatus</i>		0.4
<i>Ceratophyllum demersum</i>		0.1
<i>Hydrilla verticillata</i>		0.1
<i>Myriophyllum verticillatum</i>		0.1
<i>Batrachium trichophyllum</i>		0.1
<i>Marsilium quadrifolia-Callitriche brutia</i>		0.1
<i>Potamogeton nodosus</i>		0.1

1345

1346

1347 Table 5: Radiocarbon dates of Amirkola Lagoon

core	depth in cm	dated material	lab n°	^{14}C yr BP	calibrated age (1 σ)	$\delta^{13}\text{C}$ ‰
HCGL02	63-62	<i>Alnus</i> wood	Poz23314	150 \pm 25	AD1779-1727 or AD 1750 (1)	n/a
HCGL04	60-58	shells	UB15740	379 \pm 25	too young (2)	-2.3

1348

1349 (1) intcal04.14C, Reimer et al., 2004

1350 (2) marine04.14C, Hughen et al., 2004

1351

1352

1353 **Captions**

- 1354 Fig. 1: Location maps
 1355 1a: Location of the lagoons of Anzali and Amirkola and the main inflows
 1356 to the Caspian Sea.
 1357 1b: Location of the Caspian Sea in relation to neighbouring countries
 1358 with main sites cited in the text (asterisk), GNP = Golestan National
 1359 Park; KBG = Kara-Bogaz Gol.
- 1360 Fig. 2: Vegetation map of Amirkola Lagoon and its surrounding with location
 1361 of cored sequences and surface samples.
- 1362 Fig. 3: Vegetation map of Anzali Lagoon with core locations.
- 1363 Fig. 4: The climate along the north Iranian coast.
 1364 4a: Annual mean precipitation (in shades of grey) calculated from monthly
 1365 means by GPCC ([Rudolf et al., 2003](#)) on a half degree grid (units: mm
 1366 month⁻¹) overlaid by the orography in contours. The dashed line shows
 1367 the 2000 m topographic height contour. The position of the
 1368 meteorological stations is indicated by markers. Circles: ANZ = Anzali,
 1369 RAS = Rasht, LAH = Lahijan, RAM = Ramsar, AST = Astara, BAB =
 1370 Babolsar, TOR = Torkaman, ZAN = Zanzan; plusses: PIL = Pilimbra-
 1371 Nehalestan, MAN = Manjil, GOR = Gorgan.
 1372 4b: Annual cycle of precipitation (pre) and temperature (T2m), or Koeppen
 1373 diagrams, for the meteorological stations shown in fig. 4a by circle
 1374 markers. Data are provided by the Iran Meteorological Organization
 1375 (www.irimo.ir/english); the averages are taken for the longest time
 1376 available, at least 10 years. Ordinate on the left: precipitation in mm
 1377 month⁻¹, on the right: temperature in °C.
 1378 4c: Surface wind during autumn (SON) from ERAinterim (ERAin), a more
 1379 modern and higher resolution than the ERA40 reanalysis by the ECMWF
 1380 but with a shorter time span, overlaid by orographic height contours. The
 1381 arrow lengths are proportional to the wind speed. The maximum speeds
 1382 are 3 m s⁻¹ and typical values in the highlands SW of Anzali are 1 m s⁻¹.
 1383 Contours of orographic height at 500, 1000, 1500 and 2000 m.
- 1384 Fig. 5: Lithological logs of the six cores from Amirkola and Anzali Lagoons
 1385 and dating elements.
- 1386 Fig. 6: Amirkola and Anzali sedimentology and magnetic susceptibility. OM =
 1387 organic matter, MS = magnetic susceptibility. * = radiocarbon dates,
 1388 thick vertical bar = radionuclide profile.
- 1389 Fig. 7: Palynological diagrams of Amirkola, core HCGL02. 10 x exaggeration
 1390 curve, dot for values lower than 5 %.
- 1391 Fig. 8: Palynological diagrams of the surface samples of Amirkola, dot for
 1392 values lower than 5 %.
- 1393 Fig. 9: Palynological diagrams of Anzali, core HCGA05. 10 x exaggeration
 1394 curve, dot for values lower than 5 %.
- 1395 Fig. 10: Block diagram of the modern coast of central Guilan (top) and the
 1396 blow-up of the two investigated lagoons as reconstructed for the high
 1397 stand of the late Little Ice Age (bottom).

1398 Fig. 11: Summary of the main results for the Amirkola and the Anzali
 1399 palynological diagrams. Thin waves on white background: weaker
 1400 marine influence, dark waves on grey background stronger marine
 1401 influence.
 1402

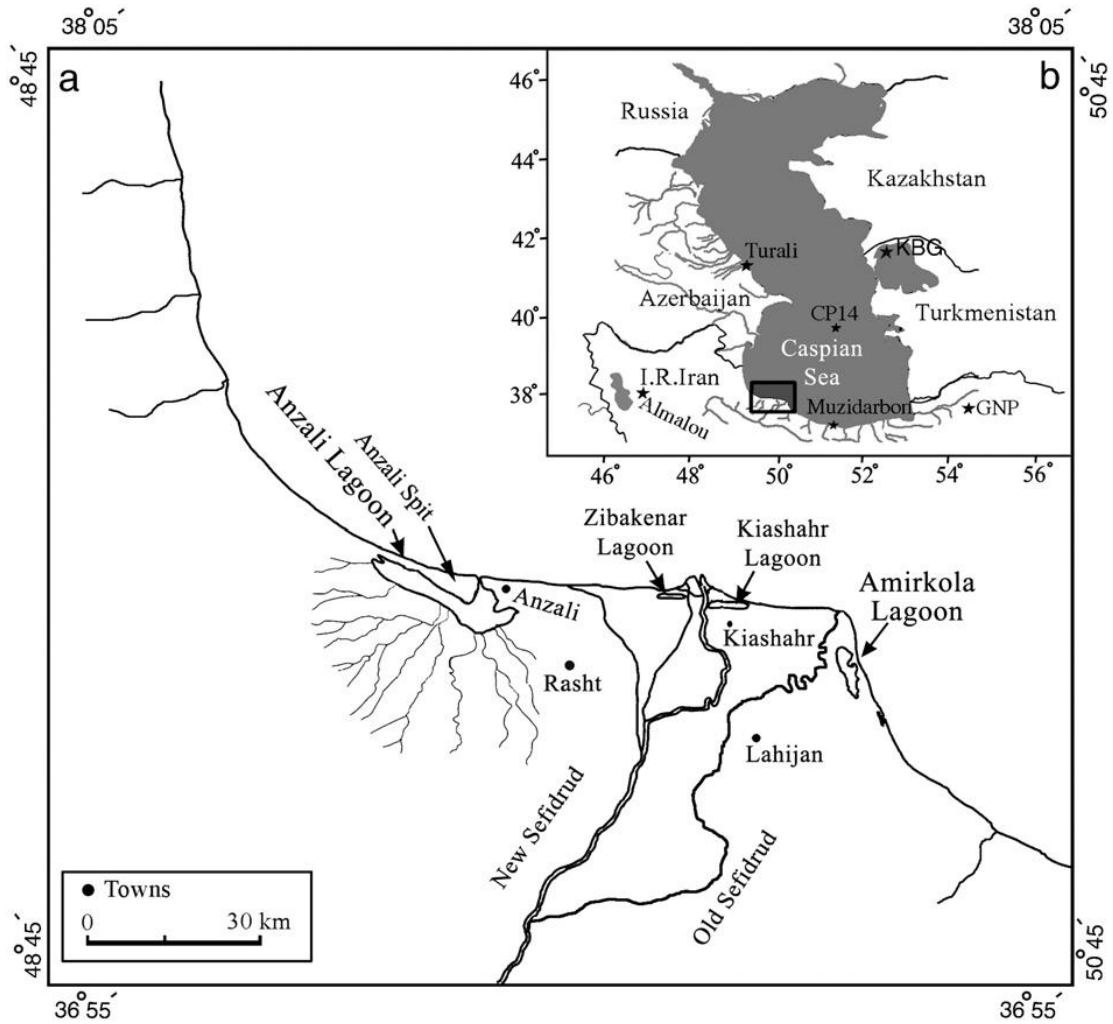


Figure 1

1403
 1404
 1405
 1406

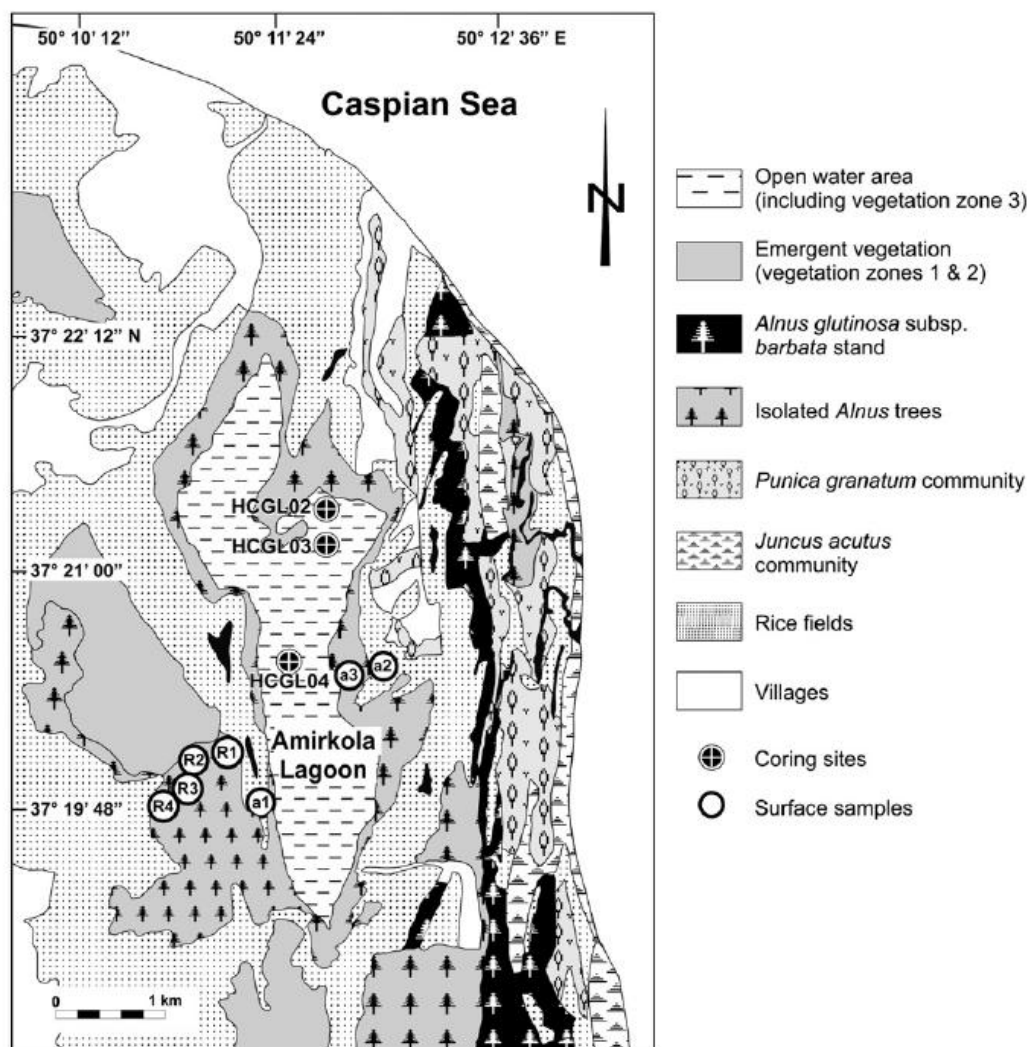


Figure 2.

1407
1408
1409
1410
1411

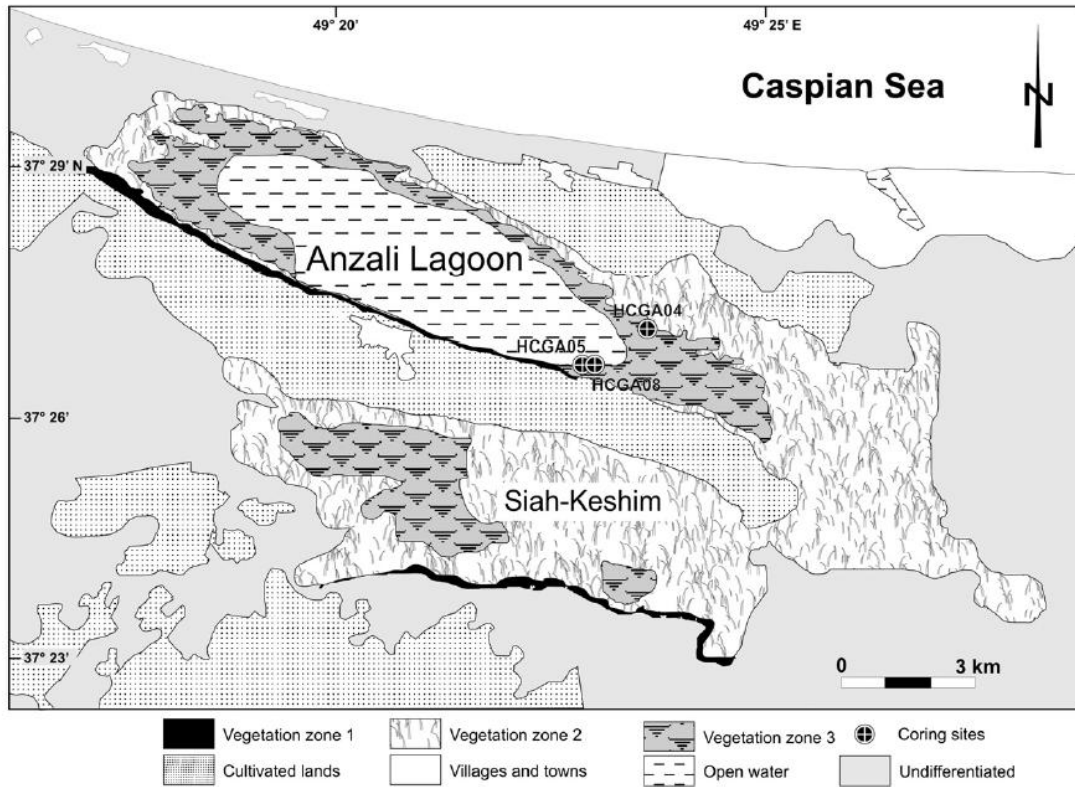


Figure 3.

1412
1413
1414
1415

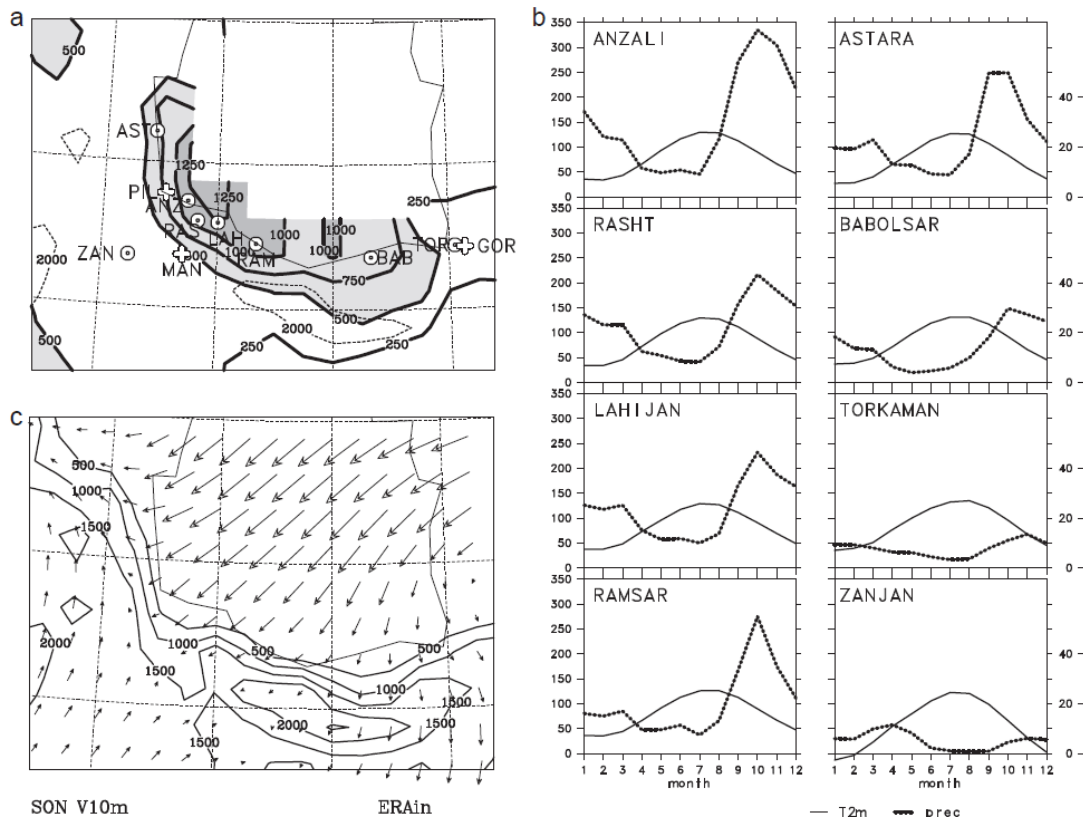


Figure 4.

1416
1417
1418
1419

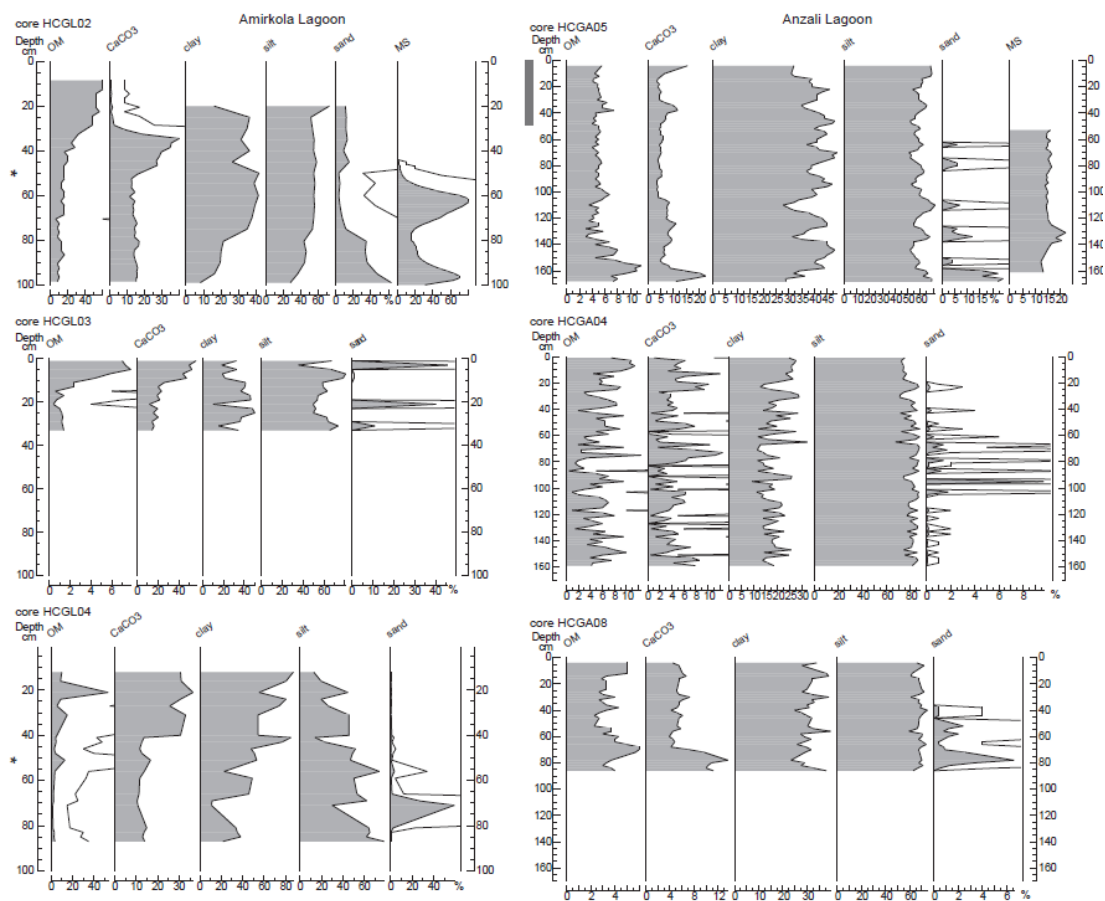
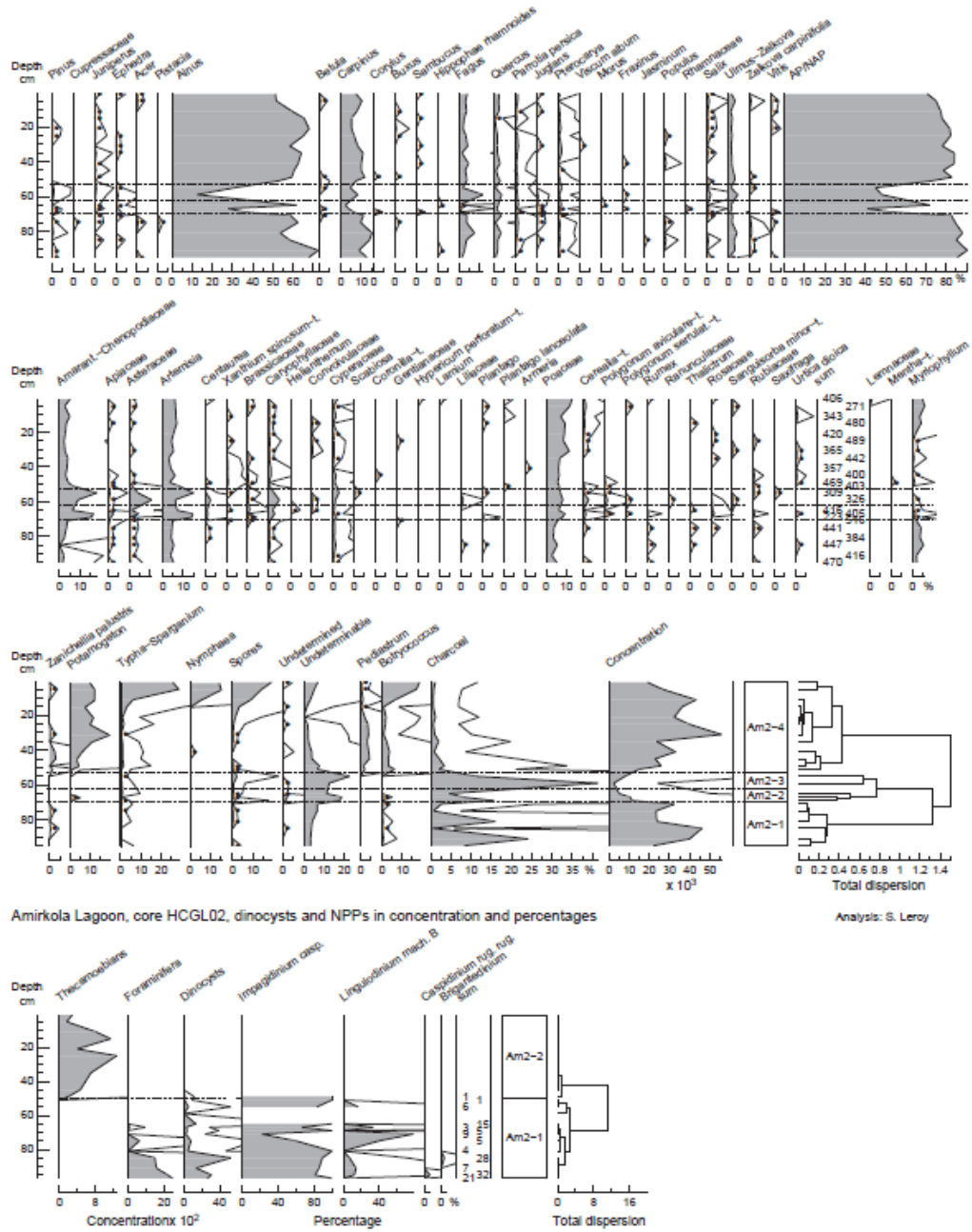


Figure 6.

1424
1425
1426
1427



1428
 1429
 1430
 1431
 1432

Figure 7

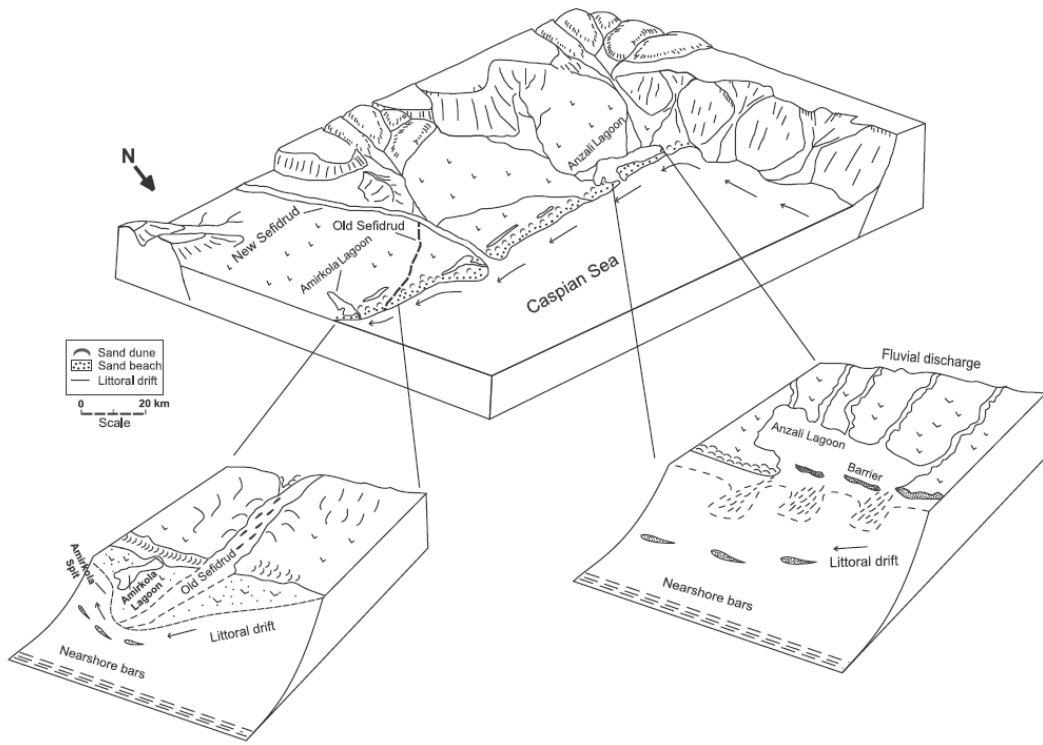


Figure 10.

1442
1443
1444
1445

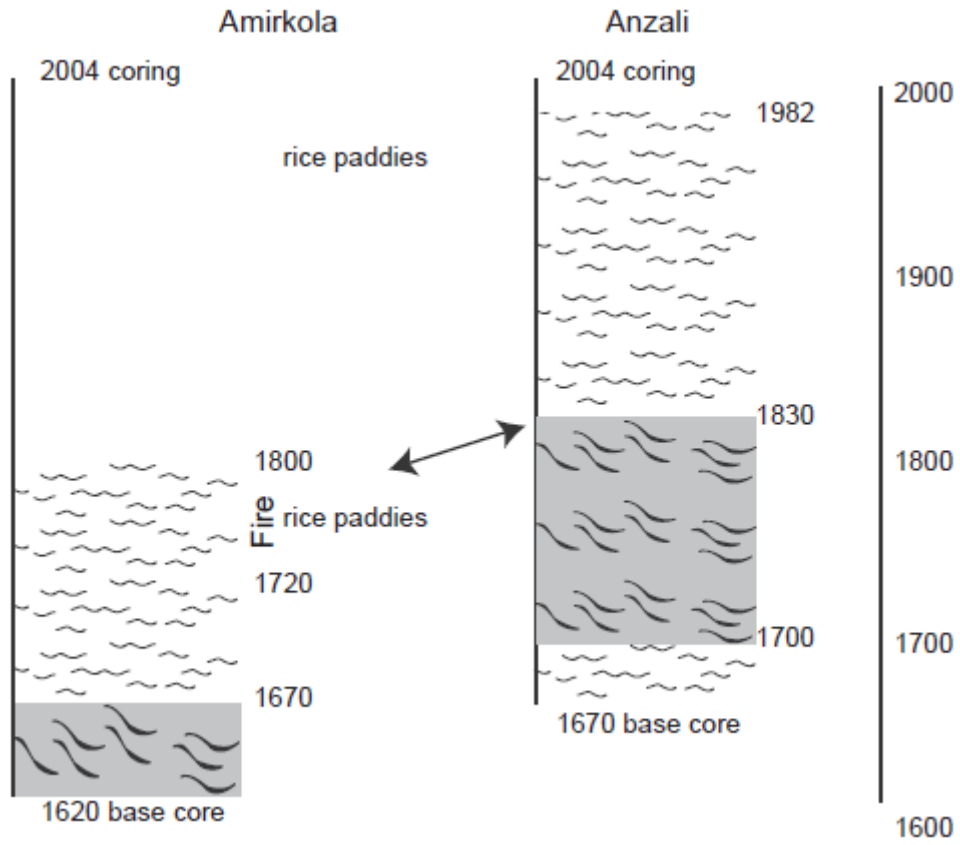


Figure 11.

1446
1447
1448
1449
1450